Understanding the Role of Flow Dynamics in Thermoacoustic Combustion Instability

Jacqueline O'Connor[a,*]

[a] *Pennsylvania State University, University Park, PA 16802*

Abstract

Thermoacoustic combustion instability is one of the most challenging operational issues in several high-performance, low-emissions combustion technologies, including gas turbines, aircraft engines, rockets, and industrial boilers. Driven by the coupling between combustor acoustics and flame heat release rate fluctuations, thermoacoustic combustion instability can lead to reduced operability, increased emissions, and, in the most extreme cases, catastrophic failure of combustor components. The feedback loop between acoustics and combustion is often facilitated by fluid mechanic oscillations, referred to as "velocity coupling," whereby acoustic oscillations drive flow fluctuations, which in turn create fluctuations in the flame. The character of these fluid mechanic oscillations is highly dependent on the structure of the flow field and the receptivity of the flow to external excitation. Combustor flow fields use features like fluid recirculation and shear to enhance flame holding and reduce emissions, but these are also the same features that can make the flow receptive to acoustic excitation or even drive self-excited oscillations. In this paper, we discuss the basics of thermoacoustic instability with a focus on the role of hydrodynamic oscillations in typical combustor flows. To facilitate this discussion, we explore the hydrodynamic instability characteristics of several key combustor unit flows (wakes, swirling jets, etc.) and show how the hydrodynamic stability of a flow is an important consideration in determining a combustor's propensity for thermoacoustic oscillations. Several examples of coupling between hydrodynamics and thermoacoustics are discussed to illustrate this important link. The paper concludes by discussing the potential for "designing" flow fields that are thermoacoustic instability resistant, either through a reduction in the receptivity of the flow or through nonlinear coupling mechanisms by which self-excited flow instabilities can suppress velocity-coupled combustion oscillations.

Keywords: Thermoacoustic combustion instability; Hydrodynamic instability; Velocity coupling

1. Introduction

Thermoacoustic combustion instability has a long history of degrading operability in combustion devices. Driven by the coupling between combustor acoustics and flame heat release rate oscillations, combustion instability has appeared in numerous combustor configurations, including rockets, power-generation gas turbines, aircraft engines, industrial boilers, and water heaters. The underlying theory is attributed to Lord Rayleigh [1], who indicated that energy could be transferred from an oscillating source of heat to an acoustic mode, and visa versa, if the two oscillated in phase. This phase relationship was later formalized by Putnam [2], as will be described in Sec. 2.

Research in the area of combustion instability gained momentum during the space race in the 1960's and 1970's as high-intensity instabilities appeared in a range of space technologies, from the mighty F-1 rocket engine (power for the Saturn V rocket) [3] to the small but safety-critical stabilization thrusters on the lunar module [4]. Instabilities appeared in solid rocket motors too, many instances of which are reviewed by Price [5]. Significant experimental [6] and theoretical [7, 8] efforts during this time laid the foundation for the modern study of thermoacoustic combustion instability and had wide-reaching implications for combustion science in general. Reviews by DeLuca and Summerfield [9], Yang and Anderson [10], and Harrje and Reardon [11] provide detailed accounts of the significant contributions to the field during this era.

The fast pace of aerospace technology development during this time also uncovered the potential for combustion instability in aircraft engines, particularly in augmentors or afterburners. Early work by Zukoski [12] on flame stabilization and Rogers and Marble [13] and Lewis [14] on flame instability identified the main mechanisms of instability in these systems. Vortex shedding from the trailing edge of the bluff body used to stabilize the flame was identified as the main coupling mechanism between the acoustic mode and flame oscillations. Instabilities in these systems had both longitudinal (referred to as "buzz") [15–17] and transverse (referred to as "screech") [18] modes.

The field enjoyed a renaissance starting in the 1990's with the introduction of dry low-NO_x (DLN) combustion systems in power-generation gas turbine engines. Motivated by increasingly stringent criteria pollutant regulations, the development of the DLN combustion system was a huge achievement for combustion science and engineering [19–23]. In these systems, reducing NO_x emissions without sacrificing power or efficiency is achieved through the use of partially-premixed combustion, sometimes called "technically-premixed combustion." Fuel is injected upstream of the flame and swirling flow is used to rapidly mix the fuel and air ahead of the inlet, producing a relatively spatially-uniform fuel/air mixture at the flame [24]. NO_x formation is not only prevented by the lack of "hot spots" in the flame, but also by the lean fuel/air mixtures typically run in these engines [25]. While NO_x can be reduced to single-digit part-per-million levels using this technology [26], this lean, partially-premixed combustion strategy has several drawbacks.

The first issue with partially-premixed combustion is flame stabilization, or "static stability," as the flame is consistently operated close to its lean extinction limit. Significant perturbations to the flame from transient compressor operation [27] or variations to fuel composition can cause the flame to blowoff [28], requiring a complex and potentially damaging restart procedure in the engine. The static stability issue has been largely resolved through creative flow design [29], online monitoring [30], and operational strategies [31, 32]. Swirling flows not only rapidly mix fuel and air, they also promote high levels of recirculation, which helps to stabilize the flame by providing regions of hot, radical-filled gases to "back-support" the flame [33, 34]. Further, online monitoring for low-frequency signals that precede flame blowoff are routinely used by engine operators to avoid this issue during operation [35, 36].

The fact that the flames are operated so close to their lean extinction limit also makes them very susceptible to incoming perturbations, which causes the second major issue with partially-premixed combustion systems. Combustion instability is much more likely in these systems as a result of this inherent flame sensitivity [37]. In gas turbine combustion systems, there are typically two coupling mechanisms that dominate the thermoacoustic feedback cycle [38]: velocity coupling and mixture coupling. Velocity coupling, which arises when acoustic oscillations drive velocity or vorticity fluctuations in the flow that they lead to flame heat release rate oscillations, has been the focus of a large number of studies [33, 39–42], including work by the author [43–46]. The other common coupling mechanism is mixture coupling, which arises when acoustic oscillations drive fluctuations in the fuel-air ratio ahead of the flame [47, 48]. One mechanism for mixture coupling arises because the fuel circuits feeding the fuel injectors are not always choked, allowing the large operability range required of these engines. As a result, acoustic oscillations in the combustor can drive fluctuations in the fuel flow rate, and in severe cases, result in acoustic resonances in the fuel system that cause very high levels of fuel flow rate oscillation. Similarly, the air flow through the compressor diffuser is not choked and so acoustic fluctuations in the combustor can drive oscillations in air-flow rate as well as the fuel-flow rate, both of which lead to variations in equivalence ratio.

One of the unifying features of the majority of combustor technologies to have experienced combustion instability is the use of complex flow fields to achieve static flame stabilization. From rocket injectors to gas turbine nozzles, fuel/air mixing and flame stabilization is achieved through the use of high levels of fluid shear and recirculation. Fluid shear is generated in a number of ways, including multiple flow passages, swirling flows, counter-swirling flows, and impinging flows. Recirculation is generated by the geometry of the combustor (typically the use of dumps or cavities) as well as the natural recirculation that appears along the centerline of swirling flows at high levels of swirl, termed "vortex breakdown."

These two flow features, however, make the flows supporting these flames susceptible to external excitation, like would be achieved in the presence of an acoustic oscillation. The dynamical features of the flows themselves are driven by their hydrodynamic instability characteristics. This review focuses on the intersection of these issues – thermoacoustic instability and hydrodynamic instability – with particular focus on low-emissions gas turbine technologies. While this review draws from many examples of current combustor configurations, next-generation combustion devices may have radically different combustor configurations to adapt to new fuels, cycles, and emissions requirements. Despite these changes, the processes driving thermoacoustic and hydrodynamic instability will not change, and so fundamental knowledge of these mechanisms is critical to continual improvement of combustion technologies.

The goal of this review is to provide a overview of the intersection of hydrodynamic and combustion instability for a broad combustion audience, recognizing that many of the topics central to thermoacoustics – acoustics, nonlinear dynamics, etc. – are not necessarily familiar to all in the combustion science community. As such, many of the details of hydrodynamic instability theory are reviewed at a high level and references are provided with more detailed discussions. We begin with brief overviews of thermoacoustic instability and hydrodynamic instability in combustor-relevant flow fields. We then explore several different facets of combustion instability issues as it pertains to hydrodynamic instability. Finally, we conclude with a discussion of the future outlook for use of hydrodynamic instability prediction tools in the design process for high-performance combustion technologies to avoid thermoacoustic instabilities.

2. Thermoacoustic Theory and Background

This section provides a short primer on thermoacoustic oscillation to support the more in-depth discussion of coupling mechanisms and combustor flows in the remainder of the paper. More details on thermoacoustic instability can be found in a number of reviews [39, 49–52].

2.1. Thermoacoustic Feedback

Thermoacoustic combustion instability is the result of a coupling between acoustic oscillations in the combustor and flame heat release rate fluctuations. Energy transfer between the flame and the acoustic field occurs when heat release rate fluctuations cause an expansion or contraction of the gases surrounding the flame, doing expansion work, $\delta W = PdV$, on the surroundings. If this work is applied to a "receptive" portion of the acoustic pressure mode, then energy can be transferred from the flame to the acoustic field. The acoustic field then produces further disturbances that can cause more heat release rate oscillations, closing the feedback loop.

This feedback loop is highly sensitive to the phase between the flame and acoustic oscillations. Even if the flame is located at a pressure anti-node, where the acoustic mode oscillation amplitude is the highest and most "receptive" to energy transfer, but the acoustic pressure and heat release rate have a phase difference of greater than 90 degrees, the energy transfer process will not occur because of this opposition. As such, the pressure and heat release rate oscillation should be within $90\deg$ phase, or a quarter of the oscillation period, in order for the energy transfer process to occur. This phase requirement is often quantified using the Rayleigh index (RI), defined in Eq. 1 and following a formulation by Putnam [2].

$$RI = \int_0^T \int_V p'(\vec{x},t)\dot{q}'(\vec{x},t)\, d\vec{x}dt \qquad (1)$$

In Eq. 1, T is the period of oscillation, V is the volume of the flame, p' is the acoustic fluctuation, and $\dot{q}'$ is the heat release rate fluctuation. The period is inverse of the acoustic frequency, $T = 1/f$, and the wavelength of the acoustic wave is related to the frequency by the speed of sound as $\lambda = c/f$. This equation indicates that if the pressure and heat release rate oscillations are within 90 degrees phase, the sign of the RI will be positive, indicating energy transfer from the flame to the acoustic field, which is a necessary but not sufficient condition for growth of the instability. A detailed discussion of the Rayleigh criterion and this phase relationship is provided by Hong et al. [53].

In order for an instability to occur, thermoacoustic driving must be greater than the damping in the system. Damping in combustion systems stems from a number of sources [54], including acoustic damping, transmission of acoustic energy out of the system, and energy lost to mechanical vibrations. The final amplitude of the oscillation is determined by the balance between the thermoacoustic driving and system damping, as is illustrated in Fig. 1, where A is the oscillation amplitude, $H(A)$ is the thermoacoustic driving, and $D(A)$ is the system damping. Oscillations will grow if the driving is greater than damping at low amplitudes, as is depicted in this sketch. The final, or "limit cycle," amplitude, A_{LC} is the amplitude where the driving and damping curves intersect. At this location, the system returns to the limit cycle regardless of whether it is perturbed to higher or lower amplitudes. If perturbed to lower amplitudes, $H(A) > D(A)$ and the system is pushed up to A_{LC}. If perturbed to higher amplitudes, $H(A) < D(A)$

and the system is pushed down to A_{LC}. This is referred to as a "stable" limit cycle, despite the fact that these oscillations are typically referred to as "combustion instability."

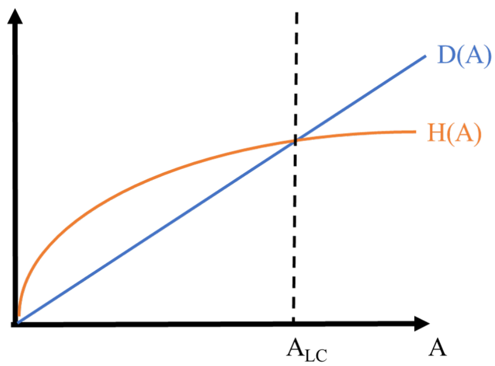

Fig. 1: Illustration of limit cycle amplitude, A_{LC}, with thermoacoustic driving, $H(A)$, and system damping, $D(A)$, as a function of instability amplitude A, following Ref. [49].

One important feature of the thermoacoustic driving curve shown in Fig. 1 is the saturation of the curve at high forcing amplitudes. While system damping typically varies linearly with oscillation amplitude, there are a number of mechanisms in the flow and flame that cause nonlinear saturation as the amplitude of heat release rate oscillation increases. These include flame cusping [55, 56], periodic changes in flame shape [57], periodic flame liftoff [58] and extinction [59], and saturating of vortex shedding strength [60]. Note that this diagram represents a vast simplification of a rich problem. Nonlinear behavior of acoustically-excited flames can vary widely, and has been discussed in a number of studies [61–64].

In reality, the coupling between the acoustic field and the flame typically includes an intermediary step, or coupling mechanism, in between the acoustic oscillation and the flame oscillation, as shown in Fig. 2. In these cases, the acoustic oscillation excites some other fluctuation in the combustion system that then leads to heat release rate oscillations. The flame still directly pumps energy into the acoustic field through the expansion work mechanism.

These coupling mechanisms introduce additional timescales and delays into the instability feedback cycle. Coupling as described by the RI only captures impact of the phase delay between the acoustic oscillation and the heat release rate oscillations. Coupling mechanisms introduce a variety of timescales that depend on the particular physics of the process. For example, many coupling mechanisms are convective processes, where the disturbance excited by the acoustic oscillation has to convect to and along the flame in order to cause the resultant heat release rate oscillation [65]. The timescale associated with the coupling mechanism is therefore related to the convective speed of the disturbance, u_c, rather than the

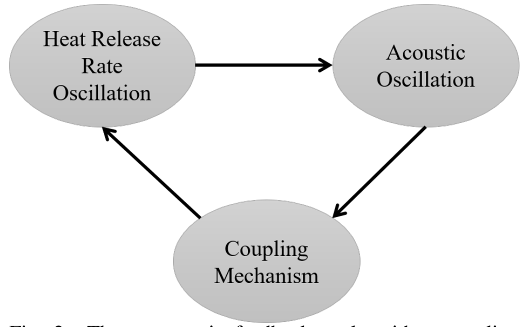

Fig. 2: Thermoacoustic feedback cycle with a coupling mechanism.

sound speed, c, where $u_c << c$ in most combustion systems. As such, the time delays associated with convective disturbances are longer and must be considered in the overall phase between heat release rate oscillations and pressure oscillations.

The impact of the delays associated with coupling mechanisms is illustrated in Fig. 3 from Gonzalez-Juez et al. [66]. Here, the instability amplitude is plotted as a function of combustor length and equivalence ratio, where varying the combustor length changes the acoustic mode shape in the combustor and varying the equivalence ratio changes the location of the flame relative to the injector. At a given combustor length, the instability amplitude varies with equivalence ratio as the flame location moves in and out of phase with the pressure anti-nodes for a given acoustic mode. The convective time delay of any disturbances in the injector, τ_c, is related to the distance of the flame from the disturbance source, X, and the convective speed of the disturbance, u_c, such that $\tau_c = X/u_c$. This convective time delay is the time it takes the coupling disturbance, in this case a vortex shed at the dump plane, to reach the flame and cause the heat release rate oscillation. The instability amplitude varies periodically with flame location (or convective delay) as the resulting phase between acoustic oscillation and heat release rate fluctuation go in and out of phase due to the additional phase delay incurred by the convective process. This phase drives the level of coupling between the acoustic field and flame, as quantified by the RI, and so the level of thermoacoustic driving changes with variations in the convective time delay. The regions of high-amplitude oscillations vary with combustor length as a result of changes to the acoustic mode shape.

One of the key features of the results in Fig. 3 is the non-monotonicity of thermoacoustic oscillation amplitude with variation in any parameter that could impact the time delay between the acoustic oscillation and the heat release rate oscillation. Any variation in a parameter that may impact the time delay between acoustics and heat release rate can result in non-monotonic variation in thermoacoustic oscillation amplitude. For example, variations in fuel composition may also change the stabilization loca-

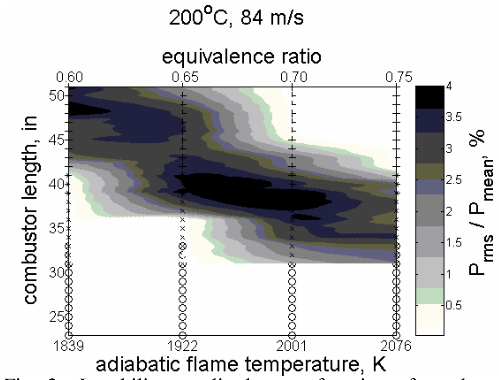

Fig. 3: Instability amplitude as a function of combustor length and equivalence ratio from Ref. [66]; reprinted by permission of the American Institute of Aeronautics and Astronautics, Inc.

tion of the flame, moving it closer to or farther away from the dump plane, changing the convection time of disturbances from the injector to the flame. Similarly, changes to the premixing hardware geometry may change the convective delay of disturbances in fuel flow rate to the flame. As such, is it impossible to definitely say whether changes in flow velocity, inlet temperature, combustor pressure, injector geometry, and a whole host of other geometric and operational parameters will have a detrimental or ameliorating effect on thermoacoustic combustion instability. The impact of these changes will always fundamentally depend on the impact of these effects on time delay, which is highly dependent on combustor geometry and operating condition.

As is evidenced by Fig. 3, the coupling mechanisms play a key role in determining the thermoacoustic stability of a combustion system. There are several coupling mechanisms pertinent to high-performance combustion system, many of which are reviewed in detail by Ducruix et al. [38]. The thesis by Shreekrishna [67] also provides detailed discussions of the physical mechanisms driving several important coupling processes. The next several sections highlight two of the main coupling mechanisms – velocity coupling and mixture coupling – as well as others that are not as highly coupled to the combustor flow field.

2.2. Velocity Coupling

Velocity coupling is the process by which the acoustic field drives velocity fluctuations in the combustor that then lead to heat release rate oscillations in the flame. The simplest example of a velocity-coupled flame is shown in Fig. 4a, which shows an acoustically-excited Bunsen flame [55]. Here, the acoustic excitation causes fluctuations in the bulk flow velocity of premixed air and fuel through the burner (shown in color), which causes periodic fluctuations in the angle of the flame at its anchoring point. These periodic fluctuations at the anchoring point arise from the fact that the flame must instantaneously meet the kinematic condition, $S_c = u_n$, where S_c is the local flame propagation speed and u_n is the velocity normal to the surface of the flame. As the bulk flow velocity oscillates due to the acoustic actuation, $u_{bulk}(t) = \bar{u} + u_a(t)'$, where $u'_a(t)$ is the acoustic velocity fluctuation, then so does the normal velocity component, resulting in a period change in the flame angle at the stabilization point. The flame wrinkle that results from the flame angle oscillation over an acoustic period convects along the flame, where its shape changes to a cusp as the flame continually propagates normal to itself, finally resulting in a rapid destruction of flame area as the cusp burns out. These oscillations in the flame area cause oscillations in heat release rate, which drive the thermoacoustic feedback cycle.

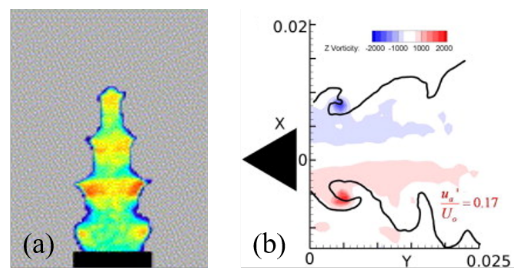

Fig. 4: Examples of velocity coupling by acoustic velocity fluctuation [55] and (b) vorticity generation [68]; reprinted with permission from Elsevier.

In more realistic combustor configurations, the velocity-coupling mechanism also acts through the excitation of vortical structures in the flow, as shown in Fig. 4b [68]. As will be described in much more detail in Sec. 3.1, flames are typically stabilized in separating shear layers, which are receptive to external excitation like that from an acoustic field. During this coupling process, the acoustic velocity fluctuation drives a vorticity fluctuation at the location of shear layer separation [69–71], forming a vortex during each acoustic period; the colors in this figure indicate phase-averaged vorticity. These vortices convect downstream, causing local wrinkling of the flame that modulates the heat release rate. Figure 4 shows this process in a bluff-body stabilized flame, where acoustic forcing drives vortex formation in the shear layer separating from either side of the bluff body [68]. Vortices shed in shear layers are not the only vortex formations that can cause velocity coupling; many other structures in these complex combustor flow fields can also contribute to the coupling process. Additionally, variations in flow velocity through a swirler can cause variations in swirl number, causing variations in flame angle as well [72]. While the major mechanism by which velocity coupling drives heat release rate oscillation is through variations in flame area, oscillations in heat release rate can also be driven by variations in flame speed due to flame stretch [73]. This stretch-driven pathway is typically only relevant at high frequencies of excitation.

2.3. Mixture Coupling

Mixture coupling, sometime referred to as "equivalence-ratio coupling," is the process by which acoustic oscillations modulate the flow of fuel and air to the flame separately, resulting in fluctuations in equivalence ratio and hence heat release rate. The mechanism by which the fuel flow is modulated is highly dependent on the configuration of the fuel injector and the fuel, particularly whether it is a gaseous or liquid fuel. For gaseous fuels, the fuel flow rate is modulated by the oscillating pressure drop across the fuel injection orifice. Inside the orifice, fuel is supplied at a constant pressure, whereas the pressure outside the orifice is fluctuating as a result of acoustic oscillations. As the fuel flow rate across the orifice is proportional to the square root of that pressure difference, the fuel flow rate oscillates with the oscillating back pressure. In certain cases, acoustic modes can couple with the fuel system, causing resonance in the fuel lines and driving very high amplitude fuel flow rate oscillations [74]. Equivalence ratio coupling can happen even with a choked fuel line, where variations in the air flow rate meet a constant fuel flow rate, resulting in equivalence ratio fluctuations at the flame.

The equivalence ratio fluctuation that reaches the flame is not the same as that generated at the fuel injection location as a result of molecular and turbulent diffusion that occurs as the disturbance convects to the flame. Work by Bluemner et al. [75] showed this effect in a swirl-stabilized methane/air flame, where tunable diode laser absorption spectroscopy (TDLAS) was used to measure methane concentrations along the length of the nozzle ahead of the flame at a range of acoustic frequencies and amplitudes. Figure 5 shows the decay in equivalence ratio fluctuation amplitude ($\hat{\phi}$) between two downstream distances with fuel-side forcing (red circles). The equivalence ratio oscillation amplitude decays faster at higher frequencies as a result of the larger spatial gradients in the local equivalence ratio since the wavelength of oscillation decreases as frequency increases. This decay is a function of the diffusivity (modeled in this work using the Peclet number), turbulence intensity, and geometry of the injector.

The variation in mixture composition drives heat release rate oscillations through a number of pathways [76]. First, oscillations in equivalence ratio cause variations in the heat of reaction, which can directly drive heat release rate oscillations. In partially-premixed flames, equivalence ratio fluctuations also drive fluctuations in flame speed, both directly or indirectly through a flame-stretch route, which can drive fluctuations in the rate at which reactants are consumed and heat is produced. The flame speed oscillations can also cause variations in flame burning area, which is the final indirect pathway by which heat release rate is modulated. These pathways can be a strong function of oscillation frequency and amplitude, and also depend on the fuel composition. A more detailed overview of these coupling pathways is described by Shreekrishna and Lieuwen [76] for partially-premixed flames. Illustrative visualization of the impact that these fuel-air oscillations can have on flames can be found in Kather et al. [77].

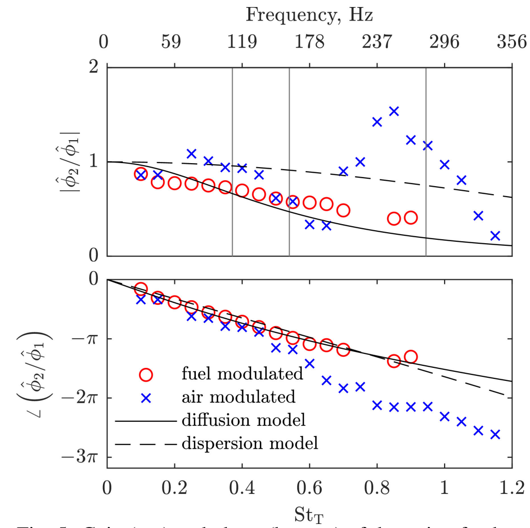

Fig. 5: Gain (top) and phase (bottom) of the ratio of coherent equivalence ratio oscillations at $x/D = 1.3$ ($\hat{\phi_1}$) and $x/D = 4$ ($\hat{\phi_2}$) as a function of forcing frequency with two model comparisons [75]; reprinted with permission from Elsevier.

The mechanisms of mixture coupling in liquid-fueled combustors are more complex than that of gaseous-fueled combustors because there are more processes with time delays between fuel injection and fuel consumption, including liquid jet breakup, atomization, and vaporization. Initially, the same governing principle driving fuel modulation in gaseous fuels applies to liquid fuels, where acoustic pressure oscillations drive fluctuations in the fuel flow rate. Work by Vogel et al. [78] showed this mechanism is sensitive to frequency, where fuel flow modulation was only observed at low frequencies and damped at high frequencies. Several studies have considered the impact of acoustic oscillations on spray breakup, including more fundamental studies [79–81] and work in aero-engine fuel injectors [82–84]. Acoustic oscillations can also impact the rate of vaporization and combustion of individual droplets. Work by Karagozian and coworkers, reviewed in Ref. [85], showed that acoustic oscillations can change the behavior of fuel droplet vaporization and burning at a range of frequencies, amplitudes, and acoustic mode shapes.

2.4. Other Coupling Mechanisms

Other coupling pathways have been identified, including pressure coupling, entropy coupling, and intrinsic instability. They are only briefly mentioned here and more thorough discussions can be found in the provided references. Pressure coupling is the direct coupling between the acoustic field and the flame, which causes heat release rate oscillations through a number of pathways. Variations in pressure at the flame drive oscillations in chemical rates and mixture density, where both these effects can drive fluctuations in heat of combustion and flame speed [73]. For pressure coupling to be important, however, acoustic oscillations must have very high amplitudes and relatively high frequencies such that the timescale of pressure modulation can impact the short timescales of chemistry. Pressure coupling can be the main driving mechanism in solid rockets [86] and some liquid rocket systems [87].

Entropy coupling is a unique coupling process, as its feedback loop has one convective leg and one acoustic leg in the feedback mechanism [88–90]. During entropy coupling, a "hot spot" from the flame, or pocket of flame products hotter than the surrounding gases, convects downstream to the exit plane of the combustor. In many combustion systems, including gas turbines and rockets, the exit plane of the combustor is nearly choked, causing a coupling between entropy and acoustic modes and generating an acoustic wave that propagates back into the combustor [91]. This acoustic wave then excites another entropy disturbance and the feedback loop continues. The frequency of this oscillation is a function of both the speed of sound and the convective velocity of the hot spots. In gas turbines, entropy coupling is observed at start-up, when the engine is relatively cold, and is referred to as "growl" or "rumble" [92]. It has also been measured in reheat combustors [93], which are more kinetically controlled rather than fluid-mechanically controlled. The flow field does have a dispersive effect on entropy disturbances, however, which can alter this complex coupling process [94–96].

Intrinsic instability is a mode of thermoacoustic combustion instability where the coupling processes occur ahead of the flame rather than in the combustor itself [97], meaning that the frequency of oscillation is decoupled from the acoustic modes of the combustor. These instabilities can exist even in combustion systems with high levels of acoustic damping, as was shown by Hoeijmakers et al. [98] in a combustor with a large horn on the downstream end and Xu et al. [99] in a combustor with a perforated acoustic liner that suppressed other thermoacoustic modes but not the intrinsic mode.

3. Combustor Flows and Instabilities

This section briefly reviews the features of common combustor flow fields and their hydrodynamic instability features. Although combustors come in many configurations, this treatment considers three canonical shapes – bluff-body flows, backward-facing steps, and swirling flows – as these geometries or combinations of these geometries appear in many combustor configurations.

3.1. Combustor Flows

Combustor flow fields are designed with the goal of stabilizing a flame over a range of operating conditions, which could result in flow velocity, equivalence ratio, and fuel composition variations [100]. In partially-premixed and premixed systems, flame stabilization is particularly challenging as flame speeds are typically much slower than the bulk flow velocity in the combustor. To resolve this kinematic issue, two fluid mechanic features are used for flame stabilization: shear and recirculation. Shear can enhance critical processes like fuel/air mixing and liquid fuel atomization ahead of the flame, but shear is also typically formed when a lower-velocity region meets a higher-velocity region of the flow, providing the flame a good place to stabilize. Shear is also generated in locations where boundary layers separate, like off the edges of bluff bodies or dumps, and these low-velocity regions are also good for flame stabilization.

Along with shear typically comes recirculation, which first occurs behind sudden expansions or ahead of sudden contractions in the area of the combustor. Several common combustor features like bluff bodies, dumps, and backwards-facing steps are used to create zones of recirculation near shear layers to help with flame stabilization. Recirculation can also be created in the central zone of swirling flows at high levels of swirl through a process called vortex breakdown. The action of recirculation helps flame stabilization by providing regions of slow-moving, hot fluid filled with chemically-active radical species in the region of flame stabilization to help support flame anchoring. These recirculation zones also back-support the flame [40, 101, 102], insulating it from heat loss to walls or cold reactant gases. Work by Coriton et al. [103–105] also showed that back-support chemically supports the flame, in addition to this thermal insulation mechanism. In the remainder of this section, brief examples of flame stabilization using these three strategies is reviewed.

3.1.1. Bluff-body stabilized flames

Bluff-body stabilized flames are used in a large number of combustion devices, including augmentors [106] and power-generation gas turbines [107]. Bluff bodies have a variety of shapes; there are both prismatic as well as cylindrical configurations. Prismatic bluff bodies are typically seen in augmentors, arranged in a circular pattern where the span of the bluff body emanates radially out from the centerline of the engine. The shape of the bluff body can take several forms [108], including a "V-gutter" [109], a ballistic shape [110], and a cylinder [35].

Figure 6 shows an image of a bluff-body stabilized flame stabilized behind a ballistic bluff body taken using CH* chemiluminescence imaging [111]. The top image shows the time-averaged flame shape and the bottom image shows an instantaneous image with an exposure time of $1/5000$ seconds. The flame is stabilized in the shear layers separating from both aft edges of the ballistic shape, and a recirculation zone region without flame is visible in between. The flame brush grows with downstream distance as turbulence from both the inflow and the shear-generated turbulence in the shear layer wrinkle the flame; flame wrinkling is particular evident in the instantaneous image. Further downstream, the flame branches move radially outward, a result of the expansion across the flames that pushes the two branches away from each other.

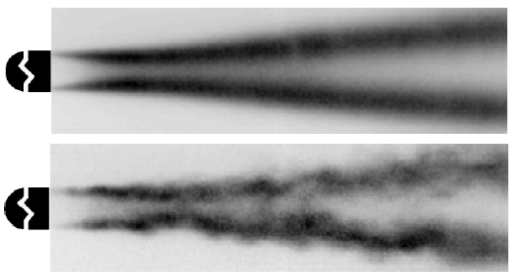

Fig. 6: Time-averaged (a) and instantaneous (b) images of a bluff-body stabilized flames on a ballistic bluff body [111]; reprinted with permission from B. Emerson.

Another common configuration for bluff-body flames is a cylindrical bluff body, as would be found in the center of a fuel-injector nozzle in a power-generation gas turbine. Figure7 shows an image of an axisymmetric flame stabilized on a bluff body [112]. Here, two examples are shown with a streamwise rod (left) and disk (right) configuration. The flame stabilizes in the shear layer separating from the trailing edge of the bluff body. Similar shape features (stabilization, downstream expansion, etc.) between the planar and axisymmetric bluff bodies are evident.

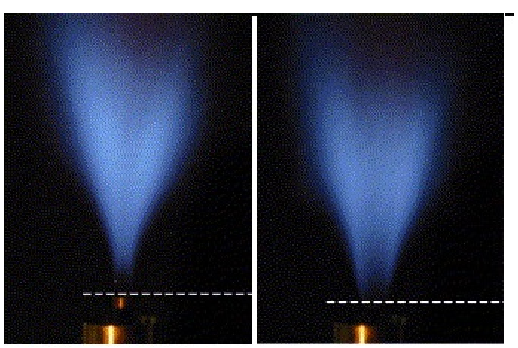

Fig. 7: Cross-section of a bluff-body stabilized flame in an axisymmetric rod (left) and disk (right) configuration [112]; reprinted with permission from Elsevier.

3.1.2. Backwards-facing steps

Backwards-facing step combustors (BFSC), or their axisymmetric counterparts called "dump combustors," capture the critical feature of area expansion in combustor design. Figure 8 shows a long-time exposure image of a flame stabilized in a BFSC [113] at three equivalence ratios, where the flame is attached at the edge of the step where the shear layer separates and stabilizes in that separating shear layer. A recirculation zone behind the step back-supports the flame, providing additional stabilization support.

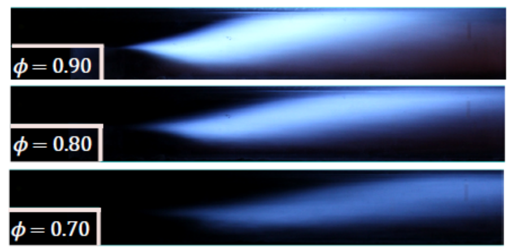

Fig. 8: Flame stabilized in a backwards-facing step combustor at three equivalence ratios [113]; reprinted with permission from S. Hong.

3.1.3. Swirl-stabilized flames

Swirl-stabilized flames can have a number of different configurations depending on the level of swirl in the flow, the presence and shape of a bluff-body, and the confinement of the flame by the outer walls of the combustor. This discussion will focus on flows with high levels of swirl, resulting in the presence of a vortex breakdown bubble. Flames can also be stabilized in flows with low levels of swirl, where the mechanism of stabilization is largely controlled by meeting the kinematic condition at the base of the flame in the central region of the flow, where the streamlines diverge and cause a low-velocity region [114]; these flames can also experience interesting combustion instability phenomena [115]. Thorough reviews of high-swirl flames is provided by Huang and Yang [39] and Candel et al. [33].

In high-swirl flows, the flow has a recirculation zone along the centerline as a result of vortex breakdown. Though there have been many explanations for the appearance of vortex breakdown in swirling flows [116–120], modern analyses [121, 122] show that early explanations by Benjamin [123] and later analyses by Darmofal [124] and Rusak and coworkers [125–127] correctly identified the mechanism as a transition from a supercritical to subcritical state in the flow. This feature produces a robust recirculation zone along the centerline of the flow, in either a bubble or conical configuration [128].

Figure 9 shows examples of the types of flame shapes achievable in a swirl-stabilized combustor [40]. First, the flame can be aerodynamically stabilized (Fig. 9I) and it forms a sort of "bowl" shape around the recirculation zone, stabilizing in this low-velocity region with significant back-support. The presence of a bluff body can cause the flame to stabilize on the downstream edge of the bluff body, resulting in a "V-flame" (Fig. 9II and III). Finally, the flame can also stabilize in the shear layers separating from the outer edge of the swirler nozzle, as shown by the "M-flame" in Fig. 9IVf and IV. Flame shapes can also change with the size and shape of the center-body [129], although the flame shapes are generally the same as those shown here.

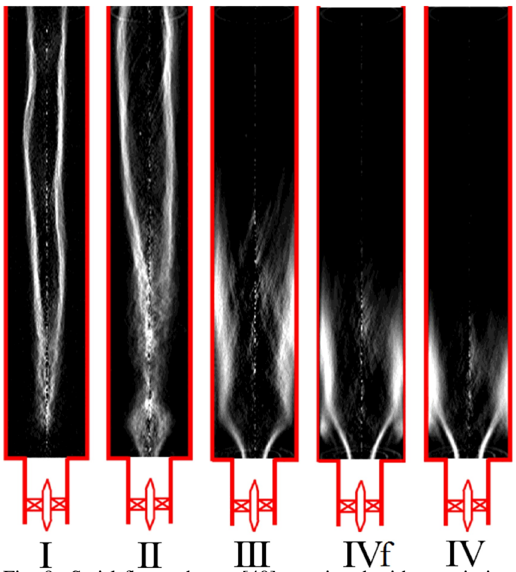

Fig. 9: Swirl flame shapes [40]; reprinted with permission from Elsevier.

3.2. Hydrodynamic Instabilities

These combustor flows, including wakes, dumps, and swirling flows, display rich fluid dynamic instabilities, referred to as "hydrodynamic instabilities." Several thorough reviews provide the detailed theory behind these instabilities [130–132], and so only an overview will be discussed here to provide the necessary background for understanding the role of hydrodynamic instability in thermoacoustic oscillations. Hydrodynamic instability is classified by the growth and propagation of infinitesimal perturbations to the flow and hydrodynamic oscillations arise when the flow is unstable. It is important to first distinguish the instability from its manifestation. The large-scale vortices or bulk oscillations that flows display when unstable are the limit-cycle oscillations resulting from the nonlinear development of a flow instability. This limit-cycle concept is the same as discussed with regards to Fig. 1. As a result, there are different categories of instabilities that can ultimate "look" the same in the flow, but have very different driving dynamics.

To begin, we will consider local stability characteristics and then build to global stability. A local stability problem makes the assumption of a "parallel" flow, where the flow profiles does not change with downstream distance, x. As such, any variations in the profile are only a function of the cross-stream direction, y. An unstable flow is one where disturbances grow, rather than decay. From a temporal perspective, a flow may be unstable if the Rayleigh inflection point theorem is met, where $d^2\bar{u}_x/dy^2 = 0$; this is a necessary but not sufficient condition. Hence, if this criteria is met, an infinitesimally small disturbance to the flow would grow to a finite level in time. This criteria only captures the linear growth of the disturbance, saying nothing of its large-amplitude behavior or saturation, and only applies to inviscid flows, but is a useful framework for determining whether disturbances to a flow will grow or decay.

Solving for the stability of a flow profile, or a "base flow," is done by constructing an eigenvalue problem from a perturbation of the governing equations of motion [130]. For example, linearly unstable modes could by identified by linearizing the Navier-Stokes equations and applying the proper boundary conditions to calculate a dispersion relation, $D(k, \omega) = 0$, where k is the wavenumber and ω is the frequency of the disturbance. Depending on whether the instability problem is formulated in space or time (or both), k and ω can be complex: $k = k_r + ik_i$ and $\omega = \omega_r + i\omega_i$. Here the real part indicates the wavenumber or frequency of oscillation and the imaginary part indicates the growth rate. The solution takes the form of $u'(x, y, t) = Real[\hat{u}(y)e^{ikx}e^{-i\omega t}]$, where $\hat{u}(y)$ is a complex quantity describing the oscillation in frequency space. While disturbance waves of several frequencies can be created by the initial perturbation, one has the largest growth rate (k_i in space, ω_i in time), which is the instability that will manifest. This fastest growing wave has a characteristic frequency and wavelength, related by the dispersion relation. A group speed is defined as $\frac{d\omega}{dk}$ and describes the propagation speed of the instability waves.

Local instabilities fall into two categories – convective instabilities and absolute instabilities [132]. Convective instabilities are those whose unstable waves travel at a group speed slower than the local convective speed of the flow, which means that the resulting disturbance is convected downstream as it grows in time. A stationary observer would see the disturbance propagate away from the source and grow in space, but the amplitude at the source location would not grow in time. Absolute instabilities are those whose disturbance waves have group speeds greater than the local convective velocity such that a stationary observer at source location would see the instability grow in time with disturbance waves propagating both forward and backward from the source.

One of the key consequences of whether a flow profile is convectively or absolutely unstable is how it responds to external excitation. Absolutely unstable flows can be self-excited, where the disturbance wave travels backwards. After the initial infinitesimal disturbance at the source location, the flow is continually able to "re-perturb" the origin point and keep the instability going. For a more precise definition of absolute instability, see Pier and Huerre [133]. In practice, flows exhibit self-excited instability when a sufficiently large region of the flow is absolutely unstable;

these flows are termed "globally unstable," which is a concept that will be described later in this section.

Convectively unstable flows are not self-excited; the initial disturbance grows as it is swept away from the origin. In turbulent flows, the incoming turbulence is typically enough to provide continual perturbation to excite an instability in a convectively unstable flow, whereas absolute instability typically manifests at much lower Reynolds numbers (before turbulent transition) because of their self-excited behaviors [134]. If a convectively unstable flow is perturbed with a single frequency, like an acoustic mode, then the flow will respond at that frequency, whereas the response in an absolutely unstable flow may be very small compared to its self-excited behavior [69, 135]. These response characteristics to tonal excitation are described more in Sec. 4.1.1.

Whether a flow at a given location is convectively or absolutely unstable is not just a function of the velocity profile, but many other parameters. One of the parameters most critical in reacting flows is the density field. For example, one hydrodynamically unstable reacting flow controlled by the density profile is a pool fire, where the flow above the pool is driven by natural convection and the puffing observed in the plume is a function of the density profile as much as the velocity profile [136]. Even in high Froude number flows where buoyancy is not a driving factor, density gradients are critical to the stability of the flow. A classic demonstration of this dependence comes from Yu and Monkewitz [137], who studied the local stability characteristics of flows as a function of density ratio, $S = \rho_c/\rho_\infty$, and the backflow ratio, $\Lambda = (\bar{u}_c - \bar{u}_\infty)/(\bar{u}_c + \bar{u}_\infty)$, where ρ_c and $\bar{u}_c$ are the density and axial velocity along the centerline of the profile, and ρ_∞ and $\bar{u}_\infty$ are the density and axial velocity of the freestream flow. Variations in Λ change the velocity profile from a wake, $\Lambda < 0$, to a jet, $\Lambda > 0$, whereas S determines whether the core of the flow is low-density, $S < 1$, or high-density, $S > 1$, as compared to the freestream.

Figure 10 shows the results of this analysis as a function of S and Λ, indicating the regions of convective instability (no hashes) and two modes of the absolute instability: sinuous (horizontal hashes) and varicose (vertical hashes). Sinuous and varicose refer to the symmetry of the mode, where sinuous motions are asymmetric about the centerline, whereas varicose modes are symmetric about the centerline. For example, the puffing of a buoyant plume is a varicose mode, whereas the side-to-side oscillation of an isothermal wake is sinuous. There are two important takeaways from this result, even though this model problem has several simplifications as compared to real combustor flows. First, there is a region of convective instability where these flows are amplifiers of external perturbations over a range of operating parameters. Second, one can identify the regions where combustion-relevant flows occur, particularly low-density wakes, like would be seen in bluff-body stabilized flames. Low-density wakes are convectively unstable, whereas high-density wakes are absolutely unstable. This feature will be discussed more in the context of combustion instability in Sec 4.2.

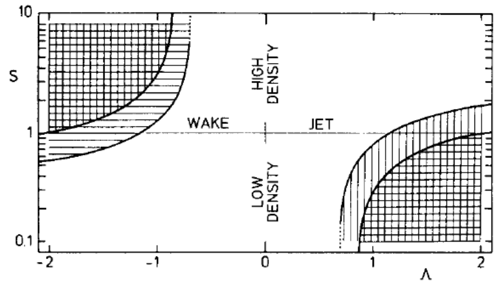

Fig. 10: Local stability of flow profiles as a function of backflow ratio, $\Lambda = (\bar{u}_c - \bar{u}_\infty)/(\bar{u}_c + \bar{u}_\infty)$, and density ratio, $S = \rho_c/\rho_\infty$ [137]; reprinted with permission from AIP Publishing.

While convective and absolute instability are useful constructs for understanding local stability, interpretation of instability changes in a spatially-developing, or non-parallel, flow. In this case, the concept of convective instability still stands, as it describes whether a disturbance will grow as it is convected away from an origin. While development of the flow profile downstream of this origin will have an impact on the local frequency and growth rate of the disturbance, whether the disturbance grows or not as it propagates away from this point is still a concept that can be applied to non-parallel flows. The concept of absolute instability, however, is much harder to apply to strongly non-parallel flows, although it does have utility in weakly non-parallel flows [130]. To be more general, we consider global instability, which is defined by a finite region of absolute instability. Key global instabilities in combustor flows are wake instabilities and the precessing vortex core, both of which are discussed next. Given this brief primer on instability theory, the next three sub-sections briefly describe the instability characteristics of the basic combustor flows described in Sec. 3.1: wakes, backwards-facing steps, and swirling jets.

3.2.1. Wake Instabilities

Wakes are formed behind flow obstructions, like bluff bodies, and are characterized by separating shear layers that enclose a recirculation zone. For simplicity, this brief overview will only consider planar wake geometries, but many of these same features can be applied to axisymmetric wakes. For a deeper treatment of planar wakes, consider Williamson [138]; for a deeper treatment of axisymmetric wakes, consider Refs. [139, 140]. An example of a wake flow is shown in Fig. 11 from Prasad and Williamson [141], in which visualization of the flow behind a cylindrical bluff body shows two key instability features of wake flows. First, the separating shear layers are unstable, displaying small-scale, symmetric vortex rollup on either side of the cylinder.

These shear layers are convectively unstable, and the instability is excited by the turbulence that is generated in the boundary layer ahead of its separation from the body. Downstream of the recirculation zone is a large-scale, sinuous wake instability, a manifestation of a global instability referred to as the Bernard-von Kármán instability. The scale of these instabilities is related to the controlling length scales of the problem, where vortices shed in shear layer instabilities scale with the momentum thickness of the separating shear layer, whereas the wake vortices scale with the diameter of the bluff body [130].

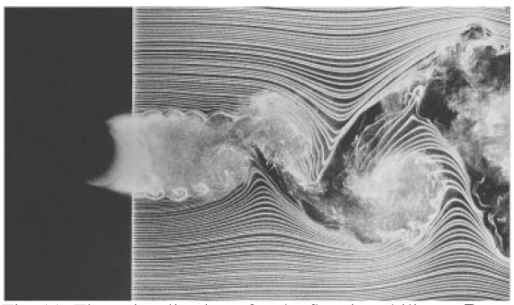

Fig. 11: Flow visualization of wake flow instability at $Re = 10,000$ [141]; reprinted from Prasad, A., Williamson, C. H. (1997). "The instability of the shear layer separating from a bluff body. Journal of Fluid Mechanics, 333, 375-402" with permission from Cambridge University Press.

3.2.2. Instabilities in Backwards-Facing Steps

The main source of instability in a backwards-facing step is the separating shear layer from the top face of the step. The instability driven by the velocity difference in these shear layers is referred to as the "Kelvin-Helmholtz" instability [131]. Details of this process are reviewed by Refs. [142–144]. This shear layer in isothermal flows is convectively unstable, resulting in vortex rollup and convection downstream. Figure 12 from Altay et al. [145] shows an acoustically-excited shear layer shedding in a backwards-facing step combustor; the visualization is of the flame over an acoustic cycle, but as the flame is stabilized in the shear layer, the vortical structures in the shear layer can be inferred from this imaging. The main length scale in the system is the step height, which drives the size of the vortex.

Another class of combustors with backwards-facing steps are those with cavities; these combustors can be found in scramjets [146] or compact engine configurations [147] and use the "trapped" vortex in the cavity to stabilize the flame. Cavities, unlike backwards-facing steps, can have a self-excited instability that arises from a convective/acoustic coupling process [148]. Here, vortices are shed from the backward-facing step at the upstream-end of the combustor and convect downstream. When they impinge on the forward-facing step at the downstream end of the cavity, the interaction between the vortex

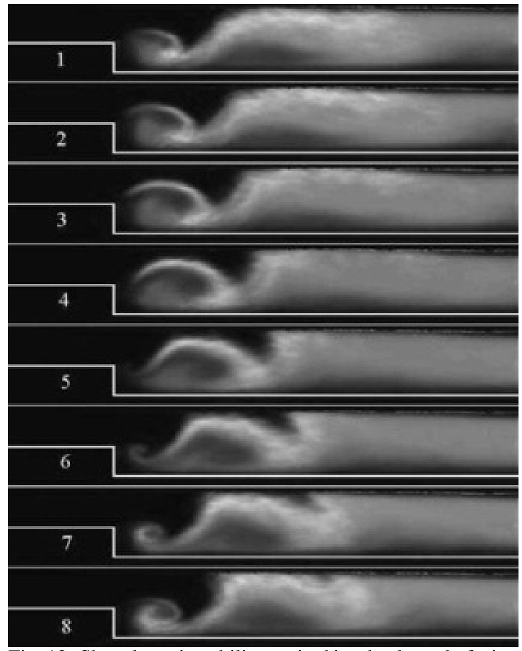

Fig. 12: Shear layer instability excited in a backwards-facing step combustor [145]; reprinted with permission from Elsevier.

and boundary creates a sound wave that propagates back upstream and excites another vortex.

3.2.3. Swirling Jet Instabilities

Swirling jets have a rich variety of instability mechanisms present, particularly in the presence of vortex breakdown. A thorough review of these mechanisms is provided by Gallaire and Chomaz [149]; instability in swirling flows has been reviewed by a number of authors [33, 150–152]. There are several instability features in swirling jets that are critical for understanding thermoacoustic instability in combustor flows, including shear layer instability, inertial waves, and the precessing vortex core (PVC). Shear layers form in two directions in swirling flows as a result of the mean shear generated by both the axial and swirling components of the flow. Shear layer instability can manifest in both directions, as has been shown in both experiments [151, 153] and theoretical predictions [118, 154].

Inertial waves have been identified in swirling flows and drive a number of different structural and oscillatory behaviors, including vortex breakdown [121, 123–125, 155–157] and oscillations in swirl number [158, 159]. Work by Albayrak et al. [158] suggests that the swirl-fluctuation mechanism of instability identified by a number of experimental studies [41, 72, 160] is the result of interaction between acoustic oscillations in the combustor and inertial waves in the swirling flow ahead of the flame.

The precessing vortex core arises from a global instability in the flow and can excite large-scale, powerful oscillations along the centerline of the flow [152]. Figure 13 from Petz et al. [161] shows a three-dimensional reconstruction of this feature. The oscillations are driven by a wavemaker, which manifests as a precession of the central core of the flow around the geometric center of the rig. This core precession excites the convectively unstable shear layers that surround the central recirculation zone, leading to the helical vortex rollup around the core. A common misunderstanding is that the PVC is the helical shear layer rollup – this is not the case. The manifestation of the instability is the core precession and the shear layer rollup is a result of the precession; the strength of the shear layer oscillations scales with the strength of the precession oscillation, as was shown by Manoharan et al. [121]. In identifying a PVC from a modal decomposition of velocity data, like a proper orthogonal decomposition [162], a PVC has both a central oscillatory region and the iconic helical shear layer oscillations. Care should be taken when identifying these structures, as the precessing vortex core can retreat upstream into the nozzle and out of view of a velocity measurement at high swirl numbers [121, 163]. Helical instabilities can exist without the presence of a PVC as a result of the shear layer instability in swirling flows [149], and so not all helical instabilities are the result of a PVC.

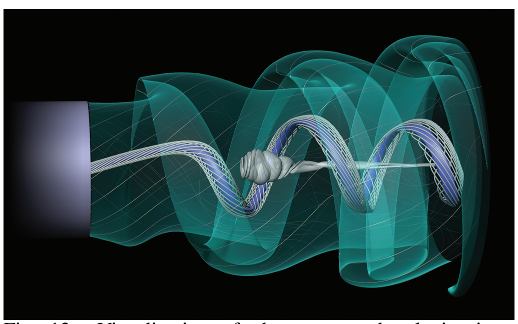

Fig. 13: Visualization of phase-averaged velocity in a swirling flow undergoing precession [161]; reprinted with permission from AIP Publishing.

4. Role of Flow Dynamics in Combustion Instability

With the background on thermoacoustic and hydrodynamic instabilities established, we can now consider the critical ways they intersect and couple in typical combustor flows. In this section, we discuss three topics: the role of hydrodynamic instability in velocity coupling processes, the impact of flames on hydrodynamic instabilities and how these may in turn change the thermoacoustic behavior of the combustion systems, and issues related to nonlinear coupling between hydrodynamic and thermoacoustic modes.

4.1. Hydrodynamic Instability and Velocity Coupling

In this section, we return to the issue of velocity coupling and consider it through the lens of hydrodynamic instability. Velocity coupling, the pathway by which acoustics drive flow oscillations that in turn drive heat release rate oscillations, is highly dependent on the stability characteristics of the flow. In particular, the concept of flow receptivity, or how a flow will respond to acoustic excitation, will determine the severity of a velocity-coupled instability in a combustor. Diagrams from Hemchandra et al. [164] in Fig. 14 show two pathways by which the hydrodynamic oscillations can couple with the thermoacoustic oscillations. In Fig. 14a, a self-excited hydrodynamic instability mode, like a globally unstable mode such as wake shedding or the PVC, can drive flow velocity oscillations that then lead to oscillations in heat release rate. Through the thermoacoustic energy transfer mechanism, these heat release rate fluctuations can drive acoustic fluctuations. In this case, several outcomes are possible. If the frequency of the global hydrodynamic mode, f_H, is equal to the resonant acoustic mode, f_a, then resonant forcing of the system can be achieved and high amplitudes of thermoacoustic oscillation are possible. As f_H and f_a move farther apart, this coupling weakens and thermoacoustic oscillation is less likely. The authors refer to this as the "semi-open loop" forcing condition. In this case, the Rayleigh criterion would not necessarily have to be met in order for heat release rate and pressure oscillations to occur, as the instability would be driven by the hydrodynamics, rather than a true thermoacoustic feedback cycle, as in Chakravarthy et al. [165].

Figure 14b shows the "fully closed-loop" condition where hydrodynamic oscillations are excited by the acoustic mode and the velocity-coupling pathway leads to thermoacoustic oscillation. Here, the flow acts as a disturbance amplifier and the flame responds to both the acoustic and vortical velocity fluctuations excited in the flow. In this scenario, the flow can be either convectively unstable or globally unstable, where f_H=f_a and there is direct coupling between the acoustic and hydrodynamic modes of oscillation. This coupling can be confirmed through the calculation of an adjoint hydrodynamic mode [166–168] that identifies the regions of highest sensitivity to external perturbation. In the remainder of this section, we consider several common velocity-coupled scenarios where the hydrodynamic stability of the flow directly informs the thermoacoustic stability of the system.

4.1.1. Coupling through shear layer instability

The role of shear layer instability in thermoacoustic combustion instability was identified early in the development of the field [13, 14, 18] and continues to be identified as a critical coupling pathway [169]. While simultaneous planar velocimetry and flame imaging techniques were not available early on, visualization of flame motions were quite clear – vortex shedding in the separating shear layer at the flame-stabilization location were driving thermoacoustic oscillations. The critical link be-

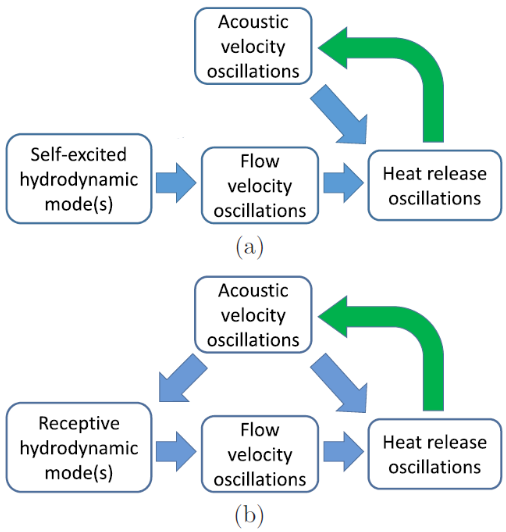

Fig. 14: Interaction of hydrodynamic oscillations with thermoacoustic feedback in (a) semi-open loop and (b) full closed-loop coupling [164]; reprinted from Hemchandra, S., Shanbhogue, S., Hong, S., Ghoniem, A. F. (2018). Role of hydrodynamic shear layer stability in driving combustion instability in a premixed propane-air backward-facing step combustor. Physical Review Fluids, 3(6), 063201. with permission from the American Physical Society.

tween the hydrodynamic stability of the flow field and velocity-coupling was established by Schadow and Gutmark [50], who related the amplitude of the heat release rate oscillations to the receptivity of the shear layer in backwards-facing step combustors. In particular, they highlighted a number of studies that showed that when the acoustic mode of the combustor matched that of the preferred shedding mode of the shear layer, velocity-coupled instability was enhanced.

Work by Hemchandra et al. [164] considered this problem with both experimental and theoretical treatments. The original experiments by Hong et al. [170, 171] used a backwards-facing step combustor at a variety of equivalence ratios, fuel compositions, and combustor lengths in order to understand the role of stretch sensitivity on velocity-coupled flame response. At a long combustor length with a fundamental acoustic mode of approximately 40 Hz, the amplitude of the thermoacoustic oscillations generally increased with increasing equivalence ratio. However, two different oscillation modes were observed with quite different flame/vortex coupling processes. At a shorter combustor length, none of the same equivalence ratios resulted in thermoacoustic oscillations.

Complementary weakly-nonlinear stability analysis was applied to base flow and density profiles fit from the experimental data. The weakly-nonlinear formulation assumes that the acoustic excitation amplitude, u_a, is much smaller than the vortical velocity fluctuation, u_ω, which measurements in most combustor configurations support. The analysis results in a method for determining whether fluctuations in the flow are driven by the acoustic or natural hydrodynamic modes, which includes a receptivity function derived from the adjoint of the solution. The solution is solved using a Wentzel-Kramers-Brillouin-Jeffreys (WKBJ) expansion [172–174], which uses a series of local stability analysis, assuming locally parallel flow, to construct a global result for a weakly non-parallel flow. The problem is solved in both space and time, and complex wavenumbers and frequencies of the solution can be determined; for more details on this solution process, see the original paper and Juniper and Pier [168].

A major result of the study is shown in Fig. 15, which shows the temporal growth rate of the shear layer mode to an impulse response at three equivalence ratios of interest with downstream distance, where the $\phi = 0.72$ mode showed moderate-amplitude thermoacoustic oscillations and the $\phi = 0.85$ mode showed large-amplitude thermoacoustic oscillations. Locations of absolute instability, indicated by $\omega_{oi} > 0$, vary significantly for the three cases, where the region over which the shear layer is absolutely unstable is much larger for $\phi = 0.72$ than $\phi = 0.85$. This result, coupled with the adjoint modes, showed that the oscillation at the $\phi = 0.72$ condition is a "semi-open loop" forcing condition, where the large region of absolute instability drives the heat release rate and pressure oscillations. However, the receptivity of the flow in the $\phi = 0.85$ case was quite high, driving very high levels of "fully closed-loop" oscillation in this case. Further, the most unstable frequency of the shear layer in the $\phi = 0.85$ mode was far from the resonant acoustic mode ($f_H \approx$ 110 Hz vs. $f_a \approx 40$ Hz), and yet it responded to the 40 Hz acoustic mode during the velocity-coupled instability. This highly coupled experimental and theoretical effort shows the subtle but critical role that hydrodynamic instability can have in driving combustion dynamics.

The concept of shear layer receptivity applies to more complex flows as well. Work by Mathews et al. [175] in a non-reacting swirling jet at various swirl numbers characterized the response of the jet to acoustic oscillations at multiple frequencies and amplitudes. The response was quantified with a vorticity transfer function, where the input was an acoustic velocity fluctuation and the output was the vorticity response in the shear layer. This initial work found that the shear layers responded strongly at low swirl numbers, but response was almost completely suppressed at high swirl numbers where a PVC formed. Follow-on work from Frederick et al. [45] showed through both experiments and local stability analysis that the PVC suppressed the response of the shear layer; this result was further confirmed in separate experiments and analysis by Lückoff et al. [176]. Calculation of the spatial growth rate of disturbances to the shear layer, using measured flow profiles, showed that when a PVC was present, the spatial growth rate

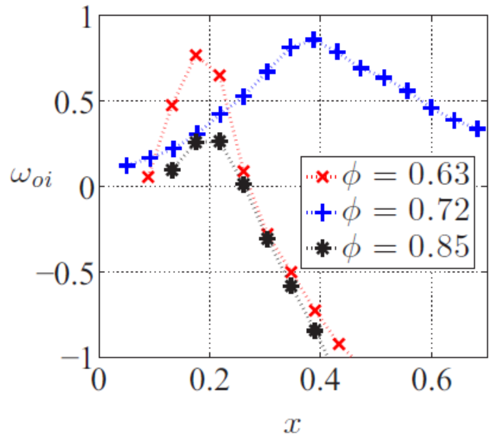

Fig. 15: Absolute growth rate of shear layer oscillations at three equivalence ratios as a function of downstream distance [164]; reprinted from Hemchandra, S., Shanbhogue, S., Hong, S., Ghoniem, A. F. (2018). Role of hydrodynamic shear layer stability in driving combustion instability in a premixed propane-air backward-facing step combustor. Physical Review Fluids, 3(6), 063201. with permission from the American Physical Society.

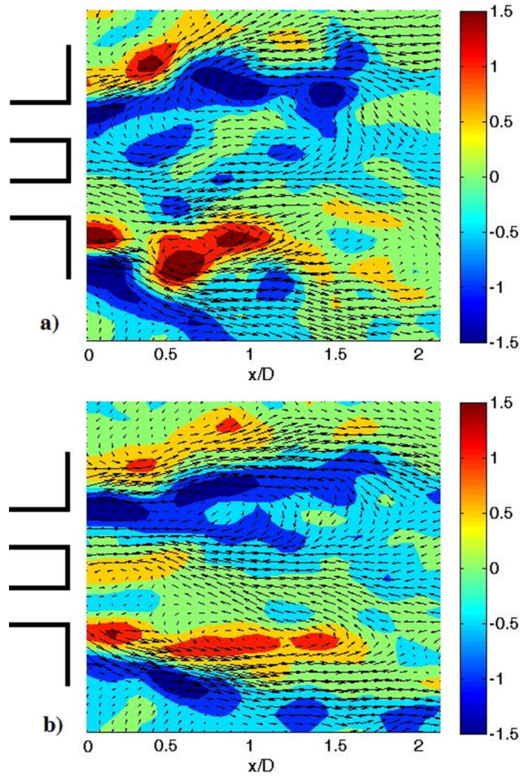

Fig. 16: Response of a reacting swirling flow to transverse forcing with (a) asymmetric and (b) symmetric transverse forcing [184]. Vectors indicate phase-resolved velocity and colorbar indicates normalized vorticity.

was negative at almost all frequencies. The action of the PVC thickened the shear layer to a point where its most receptive frequency was very low, in addition to changing the growth spatial growth rates. This work was repeated in a confined swirling jet by Mason et al. [177] and the results were again confirmed. While this study focused on non-reacting swirling jets in a gas turbine-relevant geometry, it showed the complex interactions that self-excited instabilities could have with acoustically-driven phenomena.

Shear layer response is not just sensitive to frequency, but also the symmetry of acoustic forcing. O'Connor and Lieuwen [178] experimentally investigated the impact of transverse acoustic forcing on the response of swirling flows and swirl-stabilized flames. Figure 16 shows one of the key results from this work, where Fig. 16a shows the vorticity response of the flow to a symmetric disturbance field (an acoustic velocity node/pressure anti-node) and Fig. 16b the vorticity response to an asymmetric disturbance field (an acoustic velocity anti-node/pressure node). In these figures, flow is from left to right and the transverse forcing is applied perpendicular to the direction of flow (up and down in the figure). For the symmetric forcing case, the response of both the inner and outer shear layers of the annular jet is symmetric, whereas the asymmetric forcing results in helical rollup in both shear layers. Further imaging in the radial plane confirmed this symmetry [179]. Similar results were observed by Hauser et al. [180] and Dawson and Worth [181] in experiments. Later experiments by Saurabh et al. [182, 183] continuously varied the location of the flame relative to a transverse acoustic field, with similar results.

Although the precessing vortex core in the experiments by O'Connor and Lieuwen was relatively weak as compared to the acoustically-excited shear layer dynamics [185], the natural dynamics of shear layers in swirling flow are inherently helical. Even in the absence of a PVC, the most unstable modes of the Kelvin-Helmholtz instability of the shear layer in a swirling jet is helical [186], as a result of the asymmetry introduced by the action of swirl. As such, these inherent asymmetric dynamics can appear even in the presence of symmetric forcing. Further work by O'Connor and Lieuwen [179] showed that as a ring vortex shed by a symmetric transverse excitation mode propagated downstream, it tilted, a result of the inherent asymmetry in the swirling jet.

Finally, the role of turbulence in the behavior of vortices during velocity-coupled instability should not be ignored. Work by Karmarkar et al. [187] showed that high levels of turbulence could excite coherent oscillations of a globally stable mode in a bluff-body stabilized flame, even in the absence of an acoustic mode. Similar results have been reported in non-reacting flows [167, 188], but the interaction of turbulence, the flame, and the flow instabilities is critical here. Figure 17 shows wavelet transforms of the vorticity in the shear layer just downstream of the bluff body; the signal was filtered using POD before being analyzed. The results shown are two bulk-flow velocities (5 and 15 m/s) and two inflow turbulence intensities (6% and 18%). The high turbulence intensity cases show significantly more coherent motion, which occurs at a frequency that corresponds to the BVK instability, despite the fact that the flow is globally stable because of the high density gradient introduced by the flame.

In these cases, two effects are creating this noise-driven coherent motion. First, the higher turbulence level provides larger amplitude excitation; even a highly damped system will oscillate if hit hard enough. Second, and more importantly, higher turbulence levels increase the turbulent flame speed, which increases the offset between the flame and the shear layer. As will be discussed in detail in Sec. 4.2, this offset moves the flow closer to the stability boundary of the BVK mode, increasing its receptivity to external perturbations. POD of the velocity fields in each case showed that the mode excited in the low-turbulence cases was symmetric, as the colocation of the flame with the shear layer caused significant suppression of the BVK mode. However, the POD of the high-turbulence cases showed that the noise-driven mode was asymmetric, or the BVK instability.

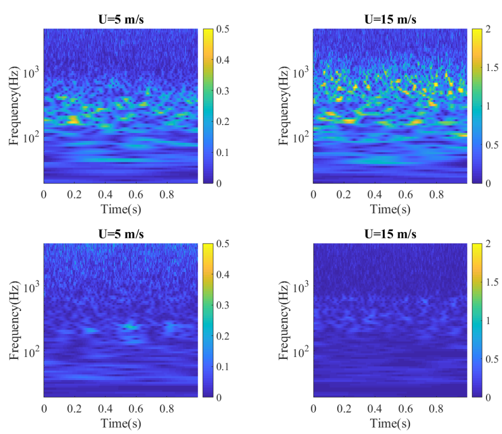

Fig. 17: Wavelet transform magnitude scalograms for the high-turbulence (top) and low-turbulence (bottom) cases at bulk velocities of 5 m/s (left) and 15 m/s (right) [187]; reprinted with permission from Elsevier.

In turbulent systems with acoustic excitation, turbulence can cause "phase jitter" in the coherent vorticity dynamics, resulting in variation in the flame's response. Work by Shanbhogue et al. [189] quantified the motion of vortex cores as a function of downstream distance at each phase in the acoustic forcing cycle for a bluff-body stabilized flame. The in-flow turbulence and the shear-generated turbulence in the bluff body shear layers caused the vortex centers to jitter from one phase to the next, reducing the coherence of the flame response.

4.1.2. Interaction of coupling mechanisms

While vortex-shedding is a critical feature of velocity-coupled combustion instability, it is not always the only velocity disturbance to drive instability. In swirl-stabilized flames, in particular, multiple velocity-coupling pathways can exist and interact with each other, resulting in non-monotonic flame response with frequency. In swirl-stabilized flames, two velocity-coupling pathways are significant: vortex shedding and swirl number fluctuations. Swirl number fluctuations arise from the interaction of acoustic oscillations and flow through the swirler, whereby the fluctuating velocity through the swirler results in fluctuations in swirl number that convect downstream to the flame [190]; Hirsch et al. [160] provide a thorough review of these mechanisms. As the origin of the swirl fluctuations and the origin of vortex formation are typically not the same, the phase between these two disturbances determines the level of velocity-coupled response of the flame. As was discussed with reference to Fig. 3, competing delay times drive the final level of thermoacoustic instability in a combustor.

Work by Palies et al. [72] showed the frequency dependence of this coupling process interference phenomenon. This experiment consisted of an axial swirler with a geometric swirl number of 0.87 at two different bulk flow velocities, $U_b = 2.67$ and $U_b = 4.13$ m/s. The flame describing function (FDF), a ratio of normalized heat release rate to normalized acoustic velocity input, was measured at a range of frequencies and amplitudes; unlike flame transfer functions (FTF), which is a linear framework for understanding flame response to disturbances, FDFs are a description of the system in both frequency and amplitude space. The heat release rate oscillations were measured using CH* chemiluminescence and the incoming flow perturbations with hot wire anemometry. Figure 18 shows the resultant FDFs for flame A at $U_b = 2.67$ m/s and flame B at $U_b = 4.13$ m/s. At all normalized forcing amplitudes, u'/U_b, a significant dip in the FDF is evident. In flame A, this dip occurs at 60 Hz, whereas it occurs at 100 Hz in flame B. In Strouhal number space, where $St = fD/U_b$, the dip occurred for both flames at $St = 0.5$, indicating that the mechanism for the dip was convective, rather than acoustic, as the normalizing velocity for St was the bulk flow velocity.

Further measurements of the velocity fluctuations at the nozzle exit showed that the acoustic excitation caused two distinct velocity disturbances: one due to vortices shed from the centerbody on which the flame was stabilized and one due to fluctuations in swirl number. At $St = 0.5$, for the given geometry of the combustor (particularly, the length between the swirler trailing edge and the centerbody trailing edge), the flame heat release rate fluctuations due to each of these two mechanisms destructively interfered, leading to a significantly lower heat release rate oscillation amplitude. Similarly, the mechanisms constructively interfered at the peaks in the FDF on

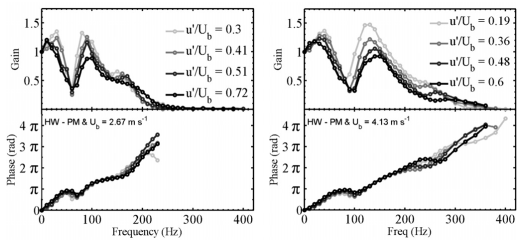

Fig. 18: Flame describing function for flame A at $U_b = 2.67$ m/s (left) and flame B $U_b = 4.13$ m/s (right) from Palies et al. [72]; reprinted with permission from Elsevier.

either side of the dip. In frequency space, this dip frequency moved because of the change in convective delay time, $\tau = L/U_b$, associated with the swirl number fluctuation traveling the distance from the swirler trailing edge to the flame, L.

A study by Bunce [191] further explored this phenomenon by changing the length of the centerbody, or location of vortex formation, relative to the fixed location of the swirler, rather than the flow velocity as was done by Palies et al. [72]. In this study, the length of the centerbody and the location of the dump plane were both modified in order to change the flame stabilization location relative to the trailing edge of the swirler, but keep the center of heat release (COHR) of the flame in the same location in the combustor. This constant COHR location is critical, as it ensures that the flame is the same place relative to the dominant acoustic mode, so that any changes to the thermoacoustic combustion instability precipitated by this change are not due to a change in the coupling described by the Rayleigh criterion, but rather changes to the velocity-coupling mechanisms. The result of this change was a shift in the minima and maxima of the FTF, just as in the work by Palies et al. [72]. The shift aligned exactly with the change in convective phase delay of the swirl fluctuation associated with the change in centerbody geometry. Recent work by Albayrak et al. [158] suggests that the source of the swirl-number fluctuations is inertial rather than convective, but the presence of multiple disturbances and their impact on the FTF is generally accepted.

4.2. Impact of Flames on Hydrodynamic Instability

In the previous section, we considered the role that hydrodynamic instability has in driving flame oscillations. However, the presence of the flame can have an impact on the behavior of hydrodynamic instability modes in combustor flows. Flames act as both sources of heat and energy in the flow, as well as regions of significant density gradients. As was discussed in Sec. 3.2, the density profile in a base flow can have a dramatic effect on the stability of the flow. Figure 10 showed this effect in the local instability of two-dimensional wakes. Density gradients can also have a significant impact on the precessing vortex core.

Simulations by Erickson and Soteriou [192] show the impact of density ratio on the Bernard-von Kàrmàn (BVK) instability in a reacting wake. Figure 19 shows variation in the vorticity (colormap) and flame (black contour) dynamics as a function of the ratio of the burnt temperature to the unburned temperature, T_b/T_u. The temperature ratio is decreased from 3.5 to 1.25 by increasing the reactant temperature; a non-reacting wake, $T_b/T_u = 1$, is shown for comparison. The density ratio, which is the physically-relevant quantity for the stability analysis, can be related to the temperature ratio through the ideal gas law. At high temperature ratios, the symmetric vortex shedding in the shear layers separating from the bluff body are visible and corrugate the flame. As the temperature ratio decreases, the asymmetric wake shedding instability arises and its inception point (or wavemaker region) moves closer to the bluff body as T_b/T_u decreases towards unity.

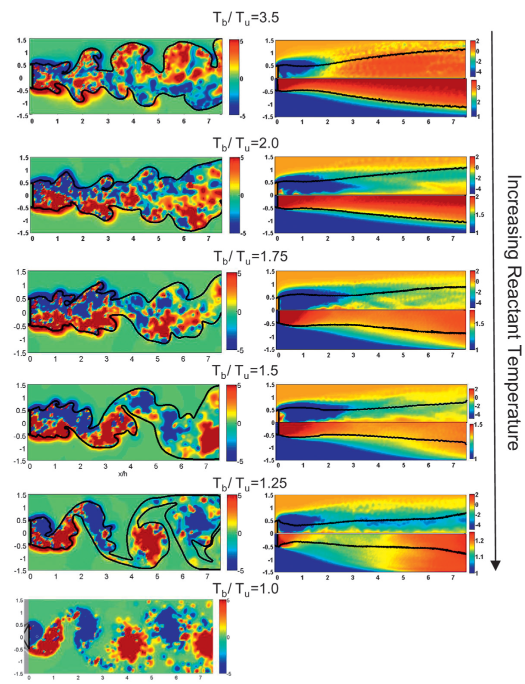

Fig. 19: Wake instability in bluff-body stabilized flame as a function of temperature ratio [192]; reprinted with permission from Elsevier.

The mechanism by which the suppression of the BVK instability occurs can be explained from both the stability analysis, as in Fig. 10, and from a vortex dynamics perspective. Vorticity dynamics are governed by convective and diffusive processes, but also by vortex dilatation, vortex stretching/bending, and baroclinic torque – where baroclinic torque is the process relevant to the interaction between the BVK instability and the flame. Baroclinic torque is generated by the misalignment of density and pressure gradients in a flow, resulting in rotation of the fluid. In a reacting flow, the density gradient is introduced by the flame and a pressure gradient arises from the low-pressure center created by the wake behind the bluff body. At high temperature gradients, baroclinic torque is generated in the opposite direction from the BVK vortices, cancelling out their formation. As the density gradient weakens as T_b/T_u approaches unity, this baroclinic effect decreases and the BVK vortices arise again.

Experiments by Emerson et al. [110] showed similar results. Here, the density ratio across a flame stabilized on a ballistic bluff body was varied using a vitiating combustor upstream, which significantly increased reactant temperature. High-speed chemiluminescence imaging was used to measure the instantaneous dynamics of the flame and high-speed PIV was used to measure the velocity profiles. The correlation coefficient between the cross-stream oscillations of either branch of the flame was used to determine whether the motion was sinuous (resulting from BVK) or varicose (resulting from KH), and this analysis showed the cross-over point from sinuous to varicose oscillations occurred at a density ratio of approximately 2.5. Local stability analysis using the measured velocity profiles supported this finding. Additional work by Rees and Juniper [193] showed the further destabilizing effect of confinement on the sinuous modes of wakes.

Further theoretical analysis by Emerson et al. [194] and simulations by Erickson and Soteriou [192] show that the relative location of the flame (density gradient) and the shear layer can have a significant impact on the flow stability. Erickson and Soteriou varied the location of the flame relative to the shear layer by changing the turbulent flame speed in the simulation, allowing the flame to propagate forward into the reactants and away from the shear layer. Figure 20 shows this effect at a temperature ratio of $T_b/T_u = 2$, which in Fig. **??** showed a complete suppression of the BVK instability. However, as the flame moves away from the shear layer, the asymmetric BVK instability reappears. From a mechanistic standpoint, the removal of the density gradient of the flame from the pressure gradient near the recirculation zone decreases the effect of the cancelling baroclinic torque. In the region where the vortices are formed, the baroclinic mechanism no longer exists and so BVK vortex shedding can occur.

Linear stability predictions from a local stability analysis by Emerson et al. [194] show the same behavior. In this analysis, a step wake profile for the velocity field and a step density profile for the flame are solved for as a function of step location of the velocity, δ_u, and density, δ_ρ, from the centerline of the flow. Figure 21 shows the normalized temporal growth rate of the instability at a given backflow ratio, $\beta = -U_b/U_u = 0.15$, where U_b is the velocity on the inside of the profile and U_u is the velocity on the outside of the profile. The quantity on the x-axis, $(\delta_\rho - \delta_u)/\delta_u$, is a normalized flame/shear offset parameter, where $(\delta_\rho - \delta_u)/\delta_u > 0$ indicates that the flame is located outside of the shear layer, which

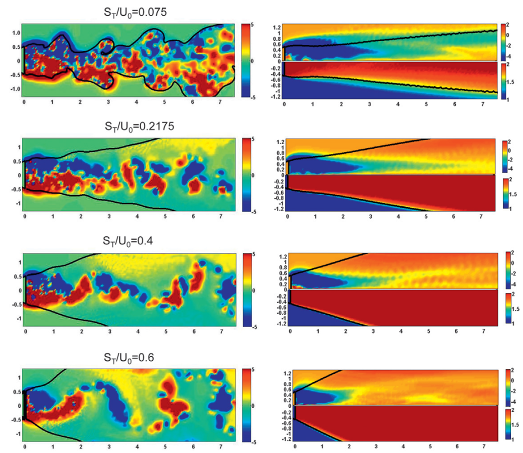

Fig. 20: Impact of turbulent flame speed on wake instability [192]; reprinted with permission from Elsevier.

would occur as turbulent flame speed increases. At co-location ($(\delta_\rho - \delta_u)/\delta_u = 0$), the growth rate is negative, for density ratios, ρ_b/ρ_u, greater than approximately 1.3. This result tracks with the results of Erickson and Soteriou [192], where flames in the shear layer suppress the BVK instability (negative growth rate). Increasing the turbulent flame speed would cause $(\delta_\rho - \delta_u)/\delta_u$ to increase, where above $(\delta_\rho - \delta_u)/\delta_u \approx 0.2$ the BVK mode is unstable again for all density ratios.

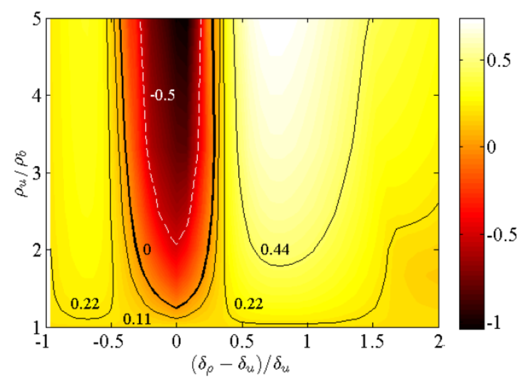

Fig. 21: Absolute instability growth rate as a function of density ratio and flame/shear offset [194]; reprinted with permission from B. Emerson.

Suppression of the PVC global mode in swirling flows has also been shown as a result of the presence of a flame. Experiments and analysis by Oberleithner et al. [195] showed that the PVC could be suppressed when a strong radial density gradient is introduced in the wavemaker region responsible for the PVC; the results were further confirmed on an industry-relevant combustor design [196]. Further local analysis by Terhaar et al. [197] showed that the PVC is most sensitive to backflow ratio and density gradient in the jet. Figure 22 shows a compilation of the results, where the contours indicate the absolute mode growth rate (left) and frequency (right), where the thick black contour indicates the boundary between convective ($\omega_0 < 0$) and absolute ($\omega_0 > 0$) instability in these cases. In these cases, a represents a backflow intensity, ρ_r is the density ratio, and q is the level of swirl, following profiles from Monkewitz and Sohn [134]. The presence of a flame affects not only the density ratio but also the backflow intensity, as expansion across the flame can significantly alter the recirculation region flow.

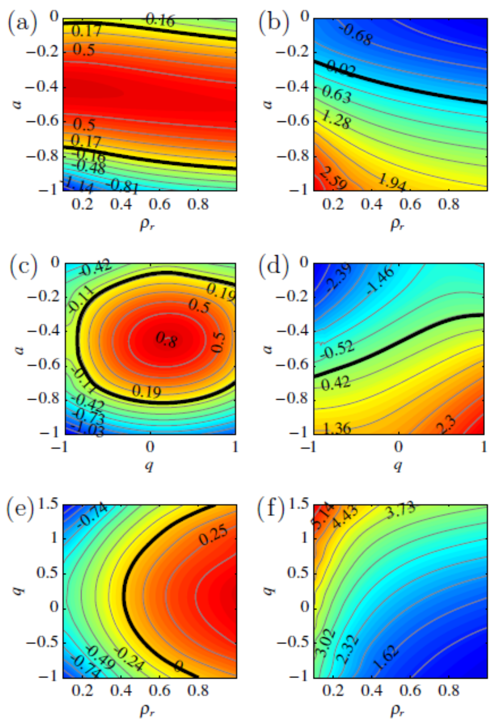

Fig. 22: Sensitivity of absolute growth rate (left) and frequency (right) of PVC to model parameters [197]; reprinted with permission from Elsevier.

Finally, the flame shape and the hydrodynamic modes are highly coupled due to the proximity of the flame stabilization point to the wavemaker region of the PVC and the shear layer separation points. A study by Stöhr et al. [198] showed the significant coupling between hydrodynamic instability, thermoacoustic instability, and flame shape. In this combustor, the flame shape intermittently oscillated between a V-flame and M-flame shape, where the center of the M-flame was lifted from the centerbody, as in Fig. 9d. A combination of experiments and local hydrodynamic stability analysis showed that a PVC was present in the M-flame configuration, but suppressed in the V-flame configuration, whereas thermoacoustic oscillations were present in the V-flame configuration but not the M-flame configuration. The transition between the two types of oscillations was precipitated by the incremental growth of the PVC mode that eventually took hold and was powerful enough to disrupt the flame shape. The M-flame did not suppress the PVC, like the V-flame, and so this transient constructive feedback cycle between flame and hydrodynamic instability was enough to change the flameholding in the combustor.

4.3. Nonlinear Coupling

Until now, we have considered largely linear coupling processes between acoustic oscillations, hydrodynamic instabilities, and the flame. Although the resultant thermoacoustic instability reaches a limit cycle oscillation amplitude, the coupling process at the shear layer separation point or in the wavemaker region is a largely a linear concept. All oscillations are occurring at the same frequency and could be predicted in a linear framework. However, there are some interesting nonlinear behaviors that can be important in the coupling between hydrodynamic and thermoacoustic oscillations in combustion systems. Note that the topic of nonlinear combuston instability is very broad and there are a large number of nonlinear behaviors in thermoacoustic systems. Here, we will consider three nonlinear behaviors that relate hydrodynamic and thermoacoustic modes – entrainment, nonlinear modal coupling, and nonlinear modal suppression – but there are many other nonlinear behaviors that could arise, including nonlinear flame response [57, 59, 61, 64, 199], instability triggering [8, 200–202], nonlinear modal coupling [203–205], among others.

Entrainment is a process by which high-amplitude external excitation changes the dynamical behavior of globally unstable flow. Emerson and Lieuwen [206] discussed this feature in the global instability of vitiated bluff-body stabilized flames where both sinuous and varicose mode components were present. A decomposition of the flame edge displacement from chemiluminescence imaging was used to determine the relative strength of the sinuous and varicose modes, where the sinuous mode was typically stabilized by the flame at high density ratios [110]. Energy from longitudinal forcing excites motion in the varicose mode, as would be expected by the symmetry of forcing vs. response. However, at forcing frequencies close to that of the BVK mode, more sinuous motion could be detected, particularly further downstream from the bluff body. When the forcing frequency is close to that of the natural mode near the bluff body, relatively equal amplification of the varicose and sinuous modes is measured. Farther downstream, however, the sinuous mode is amplified more at resonant frequencies. The unique trajectory at this condition is a result of nonlinear coupling between the forcing frequency and the sinuous response at twice the forcing frequency. Later analysis of this dataset by Pawar et al. [207] considered variations in density ratio, showing the complex temporal dynamical features that arise as the baseflow stability is varied.

Work by Moeck et al. [199] considered the impact of acoustic forcing on the precessing vortex core. A strong PVC was identified with the M-flame over a range of Reynolds numbers and equivalence ratios, and the PVC frequency was quite similar in the non-reacting and reacting conditions. Longitudinal acoustic forcing was applied at a range of frequencies and amplitudes to understand the impact acoustic forcing could have on the PVC. At certain conditions with high-amplitude forcing, spectra of both the flame (from chemiluminescence) and the flow (from laser Doppler velocimetry) show both the acoustic and hydrodynamic frequencies, as well as sum and difference frequencies, indicating nonlinear coupling. Low-frequency, high-amplitude excitation could suppress the PVC, as had been seen in previous studies [208–210]. At certain conditions, the PVC oscillated at 770 Hz and a self-excited thermoacoustic instability was present at 520 Hz. A pressure spectrum of this experiment showed a strong frequency at 250 Hz, which is the difference frequency between these two modes, indicating a strong nonlinear coupling between the two.

Another example of nonlinear coupling between a PVC and thermoacoustic instability was found in an experiment at DLR - Stuttgart, which displayed a thermoacoustic mode and a PVC at different frequencies [211, 212]. In the analysis by Steinberg et al. [211], a thermoacoustic instability at 308 Hz and a PVC at 515 Hz co-existed and created highly complex flame behaviors at both frequencies simultaneously. Figure 23 shows an example of the doubly phase resolved analysis, with the PVC at one phase and the thermoacoustic oscillation at three different phases during the same phase of the PVC. This result shows that the acoustic oscillation causes extension and contraction of the PVC structure over the acoustic cycle, and that the flame shape and location are a function of both the PVC and acoustic mode. They argue that the level of interaction between the PVC and the flame is a function of the phase of the acoustic cycle, with higher levels of interaction during maximum combustor pressure.

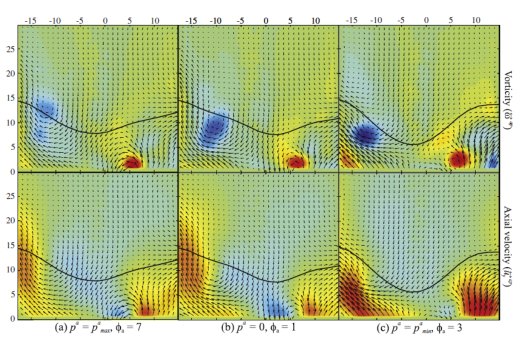

Fig. 23: Doubly phase-resolved Vorticity (top), axial velocity (bottom), and flame (contour) behavior at three phases in the thermoacoustic cycle and one phase of the PVC cycle [211]; reprinted with permission from Elsevier.

While the flame can suppress the PVC, work by Karmarkar et al. [213] showed that the PVC can suppress thermoacoustic combustion instability. In this work, a two-stream swirler nozzle with fuel injection between the two streams is used to study the impact of air split on combustor stability, where air split is defined as the the percentage of the total mass flow going through the inner passage of the nozzle. While both passages have relatively similar swirl numbers (0.82 for the inner and 0.79 for the outer), changing the air split dramatically changes the structure of the flow field. In particular, increasing the air split drives greater recirculation along the centerline and excites a PVC at an air split of 0.2 in both the non-reacting and reacting flow cases. In addition to the PVC, two thermoacoustic (TA) modes are present over a range of air splits. Figure 24 shows a key result from this experiment, where Fig. 24a shows the frequency of the three modes as a function of air split, and Fig. 24b shows the amplitude of the modes, calculated using spectral proper orthogonal decomposition [214]. The modes were identified by their shape and symmetry; the thermoacoustic modes are longitudinal modes and so excite symmetric oscillations in the flow, whereas the PVC excites a helical structure in the shear layers and has a large oscillatory region at the base of the recirculation zone.

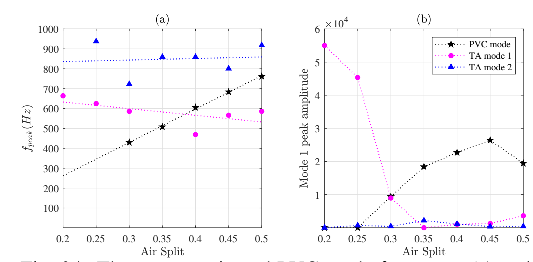

Fig. 24: Thermoacoustic and PVC mode frequency (a) and amplitude (b) as a function of air split in a dual-passage swirler [213].

The two TA modes have a relatively constant frequency as a function of air split, which would be expected for an acoustic, rather than hydrodynamic, mode. The PVC frequency increases with air split, which is expected for a hydrodynamic mode. It was determined that the PVC dynamics are driven by the flow through the central nozzle and increasing the flow split increases the flow velocity through the central nozzle, which has been shown in many previous studies to increase the frequency of PVC oscillation [152]. The key result from this analysis shows that when the PVC frequency overlaps with a thermoacoustic frequency, the thermoacoustic mode is suppressed. This occurs at air splits of 0.35-0.45 for TA1 and 0.5 for TA2. Companion weakly-nonlinear stability analysis shows that this is the result of a nonlinear interaction between the modes and that the action of the PVC suppresses shear layer response to the acoustic mode, not the other way around. This result provides interesting insight into the potential for instability suppression through hydrodynamic design.

5. Outlook for Instability Suppression

The current body of work on hydrodynamic instability and thermoacoustic instability has shown the strong link between the stability of the flow and the coupling processes in unstable combustors. Detailed experiments and simulations, when combined with stability theory, have provided deep insight into these coupling processes. The next step in the evolution of the field is to use this understanding to improve design of combustion systems and reduce the likelihood of thermoacoustic oscillations.

This concept was suggested by Juniper [215] in a discussion of instabilities in aero-engine gas turbine combustors. In this work, he applied linear stability analysis for the prediction of convective and absolute instabilities in three swirling flows: a Rankine vortex model, a single-stream swirling jet (similar to typical laboratory configurations [45, 72, 216]), and a five-stream, counter-swirling aero-engine fuel injector. In all cases, the stability theory identified the mode shapes, frequencies, and growth rates of modes in the flow. Juniper suggested that this type of analysis earlier in the design phase could help identify hydrodynamic modes with frequencies close to known acoustic resonances in the combustor, potentially leading to thermoacoustic coupling. Further adjoint analysis by Tammisola and Juniper [217] showed the opportunities for targeted suppression of a hydrodynamic mode, including those that couple with the combustor acoustics. These adjoint solutions identify potential avenues for design modification to suppress the problematic hydrodynamic oscillations.

Frederick et al. [45] came to a very similar conclusion, where we showed the pathway to combustion instability suppression through shear layer manipulation. Shear layer manipulation for suppression of noise (e.g., chevrons [218]) and other instabilities [219] is not a new concept and could be implemented in combustor geometries. For example, thermoacoustic instability in a backwards-facing step has been suppressed through suction and blowing at the step lip by Altay et al. [145]. The approach proposed by Frederick et al. [45] showed that thickening of the shear layer could reduce both its most unstable frequency to frequencies far below any resonance in the combustor, and to suppress its receptivity to external perturbations. Interestingly, the mechanisms by which this shear layer thickening was achieved was through the PVC rather than a geometric change in nozzle at the shear layer separation point or an active control mechanism [220, 221].

Promising results for the use of a hydrodynamic instability to suppress flow receptivity to thermoacoustic feedback are highlighted in work by Karmarkar et al. [213]. Here, the weakly-nonlinear framework provides a guide for more generalized instability suppression techniques. There is a potential drawback to this methodology, however. Most combustion devices operate over a range of conditions, particularly gas turbines for both propulsion and power generation, which can change the resonant frequencies in the system during operation. If the resonant frequency at a particular operating condition overlapped with that of the global mode, coupling could occur, as was shown by Boxx et al. [222]. Despite this, a clear pathway forward for the incorporation of hydrodynamic instabilities into combustor design exists.

Incorporating these lessons from hydrodynamic instability theory into the gas turbine design process is a tractable task. In the most simplistic terms, current gas turbine aerodynamic design practice is generally a three-step process: design or modification of previous designs based on empirical scalings; detailed CFD on candidate geometries; testing to confirm combustor behaviors before hardware deployment into larger engine tests. Mongia et al. [223] described the ways in which thermoacoustic considerations have traditionally been incorporated into this design process in gas turbine engines. Acoustic modeling of combustor designs at relevant operating conditions is relatively straight forward using Helmholtz solvers, and so the key frequencies of the engine are known very early in the design phase. Thermoacoustic modeling tools that incorporate measured FTFs, modeled FTFs, or other flame response models are run in parallel with CFD, as calculation of thermoacoustic instabilities in CFD is still a resource-intensive process. Recent advances, reviewed by Poinsot [224], have made these simulations more tractable.

In future, this design process could be augmented by the use of hydrodynamic instability prediction codes to better understand the potential for velocity-coupled instability in combustors. In particular, flow profiles from either empirical models or CFD could be used as input to a hydrodynamic stability code. These calculations are relatively inexpensive computationally, particularly as compared to fully unsteady CFD. Alignment between acoustic modes and hydrodynamic modes could be identified earlier in the design process and avoided through changes to the aerodynamics of the injector. This practice could be taken one step further, where design of combustors could be co-optimized for hydrodynamic instability through the use of the adjoint of the hydrodynamic modes.

The outlook is bright for the future of solving thermoacoustic instability issues in high-performance combustion systems. Our improved understanding of combustion phenomena and hydrodynamics, coupled with ever-improving simulation and experimental capabilities, has moved the science forward and opened new pathways into engineering applications.

Acknowledgments

The author's portion of this work was supported by National Science Foundation grant CBET-1749679 and U.S. Department of Energy grant DE-FE12806463 with program monitor Mark Freeman.

Any opinions, findings, and conclusions or recommendations expressed in this material are those of the authors and do not necessarily reflect the views of the National Science Foundation or Department of Energy.

I would like to recognize, with the greatest gratitude, Santosh Hemchandra for his contributions to this work. He is my longest-serving collaborator and good friend, and his deep thinking on the issues of hydrodynamic instability and thermoacoustics has been critical to my understanding of the subject. I sincerely thank the following collaborators in alphabetical order: Vishal Acharya, Michel Akiki, James Blust, Isaac Boxx, James Dawson, Benjamin Emerson, Hosam Fathy, Peter Hamlington, Fei Han, Timothy Lieuwen, Keith McManus, Bobby Noble, Stephen Peluso, Bryan Quay, Asok Ray, Domenic Santavicca, Nicholas Worth, and Yuan Xuan. I have had the privilege to work with the following students in the area of thermoacoustics: Xiaoling Chen, Sean Clees, Wyatt Culler, Evan Dillen, Daniel Doleiden, Mark Frederick, Samuel Hansford, Adam Howie, Ashwini Karmarkar, Jihang Li, Danielle Mason, Benjamin Mathews, Michael Meehan, Javier Rodriguez, Janith Samarasinghe, Olivia Sekulich, John Strollo, Ankit Tyagi, and Seth Westfall.

References

[1] J. W. S. B. Rayleigh, The theory of sound, Vol. 2, Macmillan, 1896.

[2] A. A. Putnam, Combustion-driven oscillations in industry, Elsevier Publishing Company, 1971.

[3] J. C. Oefelein, V. Yang, Comprehensive review of liquid-propellant combustion instabilities in f-1 engines, Journal of Propulsion and Power 9 (5) (1993) 657–677.

[4] T. Harmon, Apollo lunar module ascent propulsion-no second chance, in: 28th Joint Propulsion Conference and Exhibit, 1992, p. 3125.

[5] E. Price, Solid rocket combustion instability—an american historical account, Nonsteady Burning and Combustion Stability of Solid Propellants 143 (1992) 1–16.

[6] E. W. Price, Experimental solid rocket combustion instability, Symposium (International) on Combustion 10 (1) (1965) 1067–1082.

[7] F. Culick, Research on combustion instability and application to solid propellant rocket motors. ii, in: 8th Joint Propulsion Specialist Conference, 1972, p. 1049.

[8] B. T. Zinn, E. A. Powell, Nonlinear combustion instability in liquid-propellant rocket engines, Symposium (International) on Combustion 13 (1) (1971) 491–503.

[9] L. De Luca, M. Summerfield, Nonsteady burning and combustion stability of solid propellants, Vol. 143, American Institute of Aeronautics and Astronautics, 1992.

[10] V. Yang, W. Anderson, Liquid rocket engine combustion instability, Vol. 169, American Institute of Aeronautics and Astronautics, 1995.

[11] D. T. Harrje, F. H. Reardon, Liquid propellant rocket combustion instability, Scientific and Technical Information Office, National Aeronautics and Space ..., 1972.

[12] E. E. Zukoski, Flame stabilization on bluff bodies at low and intermediate reynolds numbers, Ph.D. thesis, California Institute of Technology (1954).

[13] D. E. Rogers, F. E. Marble, A mechanism for high-frequency oscillation in ramjet combustors and afterburners, Journal of Jet Propulsion 26 (6) (1956) 456–462.

[14] J. Lewis, The effect of local fuel concentration on reheat jet pipe vibrations, in: Combustion in Advanced Gas Turbine Systems, Elsevier, 1968, pp. 113–128.

[15] P. Langhorne, Reheat buzz: an acoustically coupled combustion instability. part 1. experiment, Journal of Fluid Mechanics 193 (1988) 417–443.

[16] G. Bloxsidge, A. Dowling, P. Langhorne, Reheat buzz: an acoustically coupled combustion instability. part 2. theory, Journal of Fluid Mechanics 193 (1988) 445–473.

[17] U. Hegde, D. Reuter, B. Daniel, B. Zinn, Flame driving of longitudinal instabilities in dump type ramjet combustors, Combustion Science and Technology 55 (4-6) (1987) 125–138.

[18] W. Kaskan, A. Noreen, High-frequency oscillations of a flame held by a bluff body, ASME Transactions 77 (6) (1955) 855–891.

[19] G. Leonard, J. Stegmaier, Development of an aeroderivative gas turbine dry low emissions combustion system, Journal of Engineering for Gas Turbines and Power 116 (1994) 542–546.

[20] B. C. Schlein, D. A. Anderson, M. Beukenberg, K. D. Mohr, H. L. Leiner, W. Träptau, Development history and field experiences of the first ft8 gas turbine with dry low nox combustion system, in: Turbo Expo: Power for Land, Sea, and Air, Vol. 78590, American Society of Mechanical Engineers, 1999, p. V002T02A039.

[21] L. Davis, R. Washam, Development of a dry low nox combustor, in: Turbo Expo: Power for Land, Sea, and Air, Vol. 79153, American Society of Mechanical Engineers, 1989, p. V003T06A009.

[22] K. O. Smith, Engine testing of a prototype low nox gas turbine combustor, in: Turbo Expo: Power for Land, Sea, and Air, Vol. 78958, American Society of Mechanical Engineers, 1992, p. V003T06A013.

[23] T. S. Snyder, T. J. Rosfjord, J. B. McVey, A. S. Hu, B. C. Schlein, Emission and performance of a lean-premixed gas fuel injection system for aeroderivative gas turbine engines, in: Turbo Expo: Power for Land, Sea, and Air, Vol. 78859, American Society of Mechanical Engineers, 1994, p. V003T06A008.

[24] P. Orawannukul, An experimental study of forced flame response in technically premixed flame in a lean premixed gas turbine combustor, Ph.D. thesis, Pennsylvania State University (2014).

[25] S. M. Correa, A review of nox formation under gas-turbine combustion conditions, Combustion Science and Technology 87 (1-6) (1993) 329–362.

[26] A. Manrique Carrera, P. Geipel, A. Larsson, R. Magnusson, Verification of single digit emission performance of a 24 mw gas turbine: Sgt-600 3rd generation dle, in: Turbo Expo: Power for Land, Sea, and Air, Vol. 50848, American Society of Mechanical Engineers, 2017, p. V04AT04A005.

[27] EPRI, Assessment and development of compressor health monitoring technologies (2014).

[28] S. J. Shanbhogue, S. Husain, T. Lieuwen, Lean

blowoff of bluff body stabilized flames: Scaling and dynamics, Progress in Energy and Combustion Science 35 (1) (2009) 98–120.
[29] H. Mongia, Aero-thermal design and analysis of gas turbine combustion systems-current status and future direction, in: 34th AIAA/ASME/SAE/ASEE Joint Propulsion Conference and Exhibit, 1998, p. 3982.
[30] B. Emerson, C. Perullo, T. Lieuwen, S. Sheppard, J. Kee, D. Noble, L. Angello, Combustion dynamics monitoring considerations for systems with autotuning, in: Turbo Expo: Power for Land, Sea, and Air, Vol. 51067, American Society of Mechanical Engineers, 2018, p. V04BT04A050.
[31] G. Bulat, D. Skipper, R. McMillan, K. Syed, Active control of fuel splits in gas turbine dle combustion systems, in: Turbo Expo: Power for Land, Sea, and Air, Vol. 47918, 2007, pp. 135–144.
[32] L. B. Davis, S. Black, Dry low no˜ x combustion systems for ge heavy-duty gas turbines, in: POWER-GEN Conference, 1995.
[33] S. Candel, D. Durox, T. Schuller, J.-F. Bourgouin, J. P. Moeck, Dynamics of swirling flames, Annual Review of Fluid Mechanics 46 (2014) 147–173.
[34] J. Li, H. Kwon, D. Seksinsky, D. Doleiden, J. O'Connor, Y. Xuan, M. Akiki, J. Blust, Describing the mechanism of instability suppression using a central pilot flame with coupled experiments and simulations, Journal of Engineering for Gas Turbines and Power 144 (1) (2022).
[35] S. Nair, T. Lieuwen, Acoustic detection of blowout in premixed flames, Journal of Propulsion and Power 21 (1) (2005) 32–39.
[36] S. Sarkar, A. Ray, A. Mukhopadhyay, S. Sen, Dynamic data-driven prediction of lean blowout in a swirl-stabilized combustor, International Journal of Spray and Combustion Dynamics 7 (3) (2015) 209–241.
[37] T. C. Lieuwen, V. Yang, Combustion instabilities in gas turbine engines: operational experience, fundamental mechanisms, and modeling, American Institute of Aeronautics and Astronautics, 2005.
[38] S. Ducruix, T. Schuller, D. Durox, S. Candel, Combustion dynamics and instabilities: Elementary coupling and driving mechanisms, Journal of Propulsion and Power 19 (5) (2003) 722–734.
[39] Y. Huang, V. Yang, Dynamics and stability of lean-premixed swirl-stabilized combustion, Progress in Energy and Combustion Science 35 (4) (2009) 293–364.
[40] S. Shanbhogue, Y. Sanusi, S. Taamallah, M. Habib, E. Mokheimer, A. Ghoniem, Flame macrostructures, combustion instability and extinction strain scaling in swirl-stabilized premixed ch4/h2 combustion, Combustion and Flame 163 (2016) 494–507.
[41] N. A. Bunce, B. D. Quay, D. A. Santavicca, Interaction between swirl number fluctuations and vortex shedding in a single-nozzle turbulent swirling fully-premixed combustor, Journal of Engineering for Gas Turbines and Power 136 (2) (2014).
[42] D. Fanaca, P. Alemela, C. Hirsch, T. Sattelmayer, Comparison of the flow field of a swirl stabilized premixed burner in an annular and a single burner combustion chamber, Journal of Engineering for Gas Turbines and Power 132 (7) (2010).
[43] J. O'Connor, T. Lieuwen, Disturbance field characteristics of a transversely excited burner, Combustion Science and Technology 183 (5) (2011) 427–443.
[44] W. Culler, X. Chen, J. Samarasinghe, S. Peluso, D. Santavicca, J. O'Connor, The effect of variable fuel staging transients on self-excited instabilities in a multiple-nozzle combustor, Combustion and Flame 194 (2018) 472–484.
[45] M. Frederick, K. Manoharan, J. Dudash, B. Brubaker, S. Hemchandra, J. O'Connor, Impact of precessing vortex core dynamics on shear layer response in a swirling jet, Journal of Engineering for Gas Turbines and Power 140 (6) (2018).
[46] A. Karmarkar, I. Boxx, J. O'Connor, Relative effects of velocity-and mixture-coupling in a thermoacoustically unstable, partially premixed flame, Journal of Engineering for Gas Turbines and Power 144 (1) (2022).
[47] T. Sattelmayer, Influence of the combustor aerodynamics on combustion instabilities from equivalence ratio fluctuations, Journal of Engineering for Gas Turbines and Power 125 (1) (2003) 11–19.
[48] K. Venkataraman, L. Preston, D. Simons, B. Lee, J. Lee, D. Santavicca, Mechanism of combustion instability in a lean premixed dump combustor, Journal of Propulsion and Power 15 (6) (1999) 909–918.
[49] B. T. Zinn, T. Lieuwen, Combustion instabilities: Basic concepts, in: T. Lieuwen, V. Yang (Eds.), Combustion Instabilities in Gas Turbine Engines: Operational Experience, Fundamental Mechanisms, and Modeling, American Institute of Aeronautics and Astronautics, Reston, VA, 2005, pp. 3–26.
[50] K. Schadow, E. Gutmark, Combustion instability related to vortex shedding in dump combustors and their passive control, Progress in Energy and Combustion Science 18 (2) (1992) 117–132.
[51] K. McManus, T. Poinsot, S. M. Candel, A review of active control of combustion instabilities, Progress in Energy and Combustion Science 19 (1) (1993) 1–29.
[52] J. O'Connor, V. Acharya, T. Lieuwen, Transverse combustion instabilities: Acoustic, fluid mechanic, and flame processes, Progress in Energy and Combustion Science 49 (2015) 1–39.
[53] S. Hong, S. J. Shanbhogue, R. L. Speth, A. F. Ghoniem, On the phase between pressure and heat release fluctuations for propane/hydrogen flames and its role in mode transitions, Combustion and Flame 160 (12) (2013) 2827–2842.
[54] A. P. Dowling, S. R. Stow, Acoustic analysis of gas turbine combustors, Journal of Propulsion and Power 19 (5) (2003) 751–764.
[55] A.-L. Birbaud, D. Durox, S. Candel, Upstream flow dynamics of a laminar premixed conical flame submitted to acoustic modulations, Combustion and Flame 146 (3) (2006) 541–552.
[56] D.-H. Shin, T. Lieuwen, Flame wrinkle destruction processes in harmonically forced, laminar premixed flames, Combustion and Flame 159 (11) (2012) 3312–3322.
[57] B. D. Bellows, M. K. Bobba, J. M. Seitzman, T. Lieuwen, Nonlinear flame transfer function characteristics in a swirl-stabilized combustor, Journal of Engineering for Gas Turbines and Power 129 (2007) 954–961.
[58] S. K. Thumuluru, M. K. Bobba, T. Lieuwen, Mechanisms of the nonlinear response of a swirl flame to harmonic excitation, in: Turbo Expo: Power for Land, Sea, and Air, Vol. 47918, 2007, pp. 721–731.
[59] N. Noiray, D. Durox, T. Schuller, S. Candel, A unified framework for nonlinear combustion instability anal-

ysis based on the flame describing function, Journal of Fluid Mechanics 615 (2008) 139–167.

[60] I. Weisbrot, I. Wygnanski, On coherent structures in a highly excited mixing layer, Journal of Fluid Mechanics 195 (1988) 137–159.

[61] P. Palies, D. Durox, T. Schuller, S. Candel, Nonlinear combustion instability analysis based on the flame describing function applied to turbulent premixed swirling flames, Combustion and Flame 158 (10) (2011) 1980–1991.

[62] B. D. Bellows, M. K. Bobba, A. Forte, J. M. Seitzman, T. Lieuwen, Flame transfer function saturation mechanisms in a swirl-stabilized combustor, Proceedings of the Combustion Institute 31 (2) (2007) 3181–3188.

[63] B. Ćosić, J. P. Moeck, C. O. Paschereit, Nonlinear instability analysis for partially premixed swirl flames, Combustion Science and Technology 186 (6) (2014) 713–736.

[64] R. Balachandran, B. Ayoola, C. Kaminski, A. Dowling, E. Mastorakos, Experimental investigation of the nonlinear response of turbulent premixed flames to imposed inlet velocity oscillations, Combustion and Flame 143 (1-2) (2005) 37–55.

[65] J. A. Lovett, K. T. Uznanski, Prediction of combustion dynamics in a staged premixed combustor, in: Turbo Expo: Power for Land, Sea, and Air, Vol. 36061, 2002, pp. 807–815.

[66] E. Gonzalez, J. Lee, D. Santavicca, A study of combustion instabilities driven by flame-vortex interactions, in: 41st AIAA/ASME/SAE/ASEE Joint Propulsion Conference & Exhibit, 2005, p. 4330.

[67] Shreekrishna, Response mechanisms of attached premixed flames to harmonic forcing, Ph.D. thesis, Georgia Institute of Technology (2011).

[68] S. Shanbhogue, D.-H. Shin, S. Hemchandra, D. Plaks, T. Lieuwen, Flame-sheet dynamics of bluff-body stabilized flames during longitudinal acoustic forcing, Proceedings of the Combustion Institute 32 (2) (2009) 1787–1794.

[69] D. Oster, I. Wygnanski, The forced mixing layer between parallel streams, Journal of Fluid Mechanics 123 (1982) 91–130.

[70] H. E. Fiedler, P. Mensing, The plane turbulent shear layer with periodic excitation, Journal of Fluid Mechanics 150 (1985) 281–309.

[71] C.-M. Ho, L.-S. Huang, Subharmonics and vortex merging in mixing layers, Journal of Fluid Mechanics 119 (1982) 443–473.

[72] P. Palies, D. Durox, T. Schuller, S. Candel, The combined dynamics of swirler and turbulent premixed swirling flames, Combustion and Flame 157 (9) (2010) 1698–1717.

[73] Shreekrishna, T. Lieuwen, High frequency premixed flame response to acoustic perturbations, in: 15th AIAA/CEAS Aeroacoustics Conference (30th AIAA Aeroacoustics Conference), 2009, p. 3261.

[74] G. A. Richards, E. H. Robey, Effect of fuel system impedance mismatch on combustion dynamics, Journal of Engineering for Gas Turbines and Power 130 (1) (2008).

[75] R. Bluemner, C. O. Paschereit, K. Oberleithner, Generation and transport of equivalence ratio fluctuations in an acoustically forced swirl burner, Combustion and Flame 209 (2019) 99–116.

[76] Shreekrishna, S. Hemchandra, T. Lieuwen, Premixed flame response to equivalence ratio perturbations, Combustion Theory and Modelling 14 (5) (2010) 681–714.

[77] V. Kather, F. Lückoff, C. O. Paschereit, K. Oberleithner, Interaction of equivalence ratio fluctuations and flow fluctuations in acoustically forced swirl flames, International Journal of Spray and Combustion Dynamics 13 (1-2) (2021) 72–95.

[78] M. Vogel, M. Bachfischer, J. Kaufmann, T. Sattelmayer, Experimental investigation of equivalence ratio fluctuations in a lean premixed kerosene combustor, Experiments in Fluids 62 (5) (2021) 1–14.

[79] T. Anderson, D. Kendrick, J. Cohen, Measurement of spray/acoustic coupling in gas turbine fuel injectors, in: 36th AIAA Aerospace sciences meeting and exhibit, 1998, p. 718.

[80] K. Bunce, J. Lee, D. Santavicca, Characterization of liquid jets-in-crossflow under high temperature, high velocity non-oscillating and oscillating flow conditions, in: 44th AIAA Aerospace Sciences Meeting and Exhibit, 2006, p. 1225.

[81] W. A. Chishty, U. Vandsburger, W. R. Saunders, W. T. Baumann, Interaction between thermoacoustic oscillations and spray combustion, in: Engineering Turbulence Modelling and Experiments 6, Elsevier Science B.V., 2005, pp. 865–874.

[82] T. Providakis, L. Zimmer, P. Scouflaire, S. Ducruix, Characterization of the acoustic interactions in a two-stage multi-injection combustor fed with liquid fuel, Journal of Engineering for Gas Turbines and Power 134 (11) (2012).

[83] S. Kheirkhah, J. M. Cirtwill, P. Saini, K. Venkatesan, A. M. Steinberg, Dynamics and mechanisms of pressure, heat release rate, and fuel spray coupling during intermittent thermoacoustic oscillations in a model aeronautical combustor at elevated pressure, Combustion and Flame 185 (2017) 319–334.

[84] J. J. Philo, M. D. Frederick, C. D. Slabaugh, 100 khz piv in a liquid-fueled gas turbine swirl combustor at 1 mpa, Proceedings of the Combustion Institute 38 (1) (2021) 1571–1578.

[85] A. R. Karagozian, Acoustically coupled combustion of liquid fuel droplets, Applied Mechanics Reviews 68 (4) (2016).

[86] R. Brown, R. Muzzy, Linear and nonlinear pressure coupled combustion instability of solid propellants, AIAA Journal 8 (8) (1970) 1492–1500.

[87] W. Sirignano, J. Delplanque, C. Chiang, R. Bhatia, Liquid-propellant droplet vaporization: A rate-controlling process for combustion instability, in: Liquid rocket engine combustion instability, Vol. 169, American Institute of Aeronautics and Astronautics, Reston, VA, 1995, pp. 307–343.

[88] E. Motheau, F. Nicoud, T. Poinsot, Mixed acoustic–entropy combustion instabilities in gas turbines, Journal of Fluid Mechanics 749 (2014) 542–576.

[89] L. Li, D. Zhao, Coupling between entropy and unsteady heat release in a thermoacoustic system with a mean flow, Journal of Sound and Vibration 382 (2016) 73–83.

[90] M. Howe, Indirect combustion noise, Journal of Fluid Mechanics 659 (2010) 267–288.

[91] W. Polifke, C. O. Paschereit, K. Döbbeling, Constructive and destructive interference of acoustic and entropy waves in a premixed combustor with a choked exit, International Journal of Acoustics and Vibration 6 (3) (2001) 135–146.

[92] J. Eckstein, E. Freitag, C. Hirsch, T. Sattelmayer, Ex-

perimental study on the role of entropy waves in low-frequency oscillations in a rql combustor, Journal of Engineering for Gas Turbines and Power 128 (2006) 264–270.
[93] F. Gant, A. Gruber, M. R. Bothien, Development and validation study of a 1d analytical model for the response of reheat flames to entropy waves, Combustion and Flame 222 (2020) 305–316.
[94] A. S. Morgans, C. S. Goh, J. A. Dahan, The dissipation and shear dispersion of entropy waves in combustor thermoacoustics, Journal of Fluid Mechanics 733 (2013).
[95] Y. Xia, I. Duran, A. S. Morgans, X. Han, Dispersion of entropy perturbations transporting through an industrial gas turbine combustor, Flow, Turbulence and Combustion 100 (2) (2018) 481–502.
[96] T. L. Kaiser, K. Oberleithner, A global linearized framework for modelling shear dispersion and turbulent diffusion of passive scalar fluctuations, Journal of Fluid Mechanics 915 (2021).
[97] T. Emmert, S. Bomberg, W. Polifke, Intrinsic thermoacoustic instability of premixed flames, Combustion and Flame 162 (1) (2015) 75–85.
[98] M. Hoeijmakers, V. Kornilov, I. L. Arteaga, P. de Goey, H. Nijmeijer, Intrinsic instability of flame–acoustic coupling, Combustion and Flame 161 (11) (2014) 2860–2867.
[99] L. Xu, J. Zheng, G. Wang, Z. Feng, X. Tian, L. Li, F. Qi, Investigation on the intrinsic thermoacoustic instability of a lean-premixed swirl combustor with an acoustic liner, Proceedings of the Combustion Institute 38 (4) (2021) 6095–6103.
[100] A. H. Lefebvre, Gas turbine combustion, CRC Press, 1998.
[101] Q. Zhang, S. J. Shanbhogue, Shreekrishna, T. Lieuwen, J. O'Connor, Strain characteristics near the flame attachment point in a swirling flow, Combustion Science and Technology 183 (7) (2011) 665–685.
[102] C. Foley, I. Chterev, B. Noble, J. Seitzman, T. Lieuwen, Shear layer flame stabilization sensitivities in a swirling flow, International Journal of Spray and Combustion Dynamics 9 (1) (2017) 3–18.
[103] B. Coriton, M. D. Smooke, A. Gomez, Effect of the composition of the hot product stream in the quasi-steady extinction of strained premixed flames, Combustion and Flame 157 (11) (2010) 2155–2164.
[104] B. Coriton, J. H. Frank, A. Gomez, Effects of strain rate, turbulence, reactant stoichiometry and heat losses on the interaction of turbulent premixed flames with stoichiometric counterflowing combustion products, Combustion and Flame 160 (11) (2013) 2442–2456.
[105] B. Coriton, J. H. Frank, A. Gomez, Interaction of turbulent premixed flames with combustion products: Role of stoichiometry, Combustion and Flame 170 (2016) 37–52.
[106] S. Kostka, A. C. Lynch, B. C. Huelskamp, B. V. Kiel, J. R. Gord, S. Roy, Characterization of flame-shedding behavior behind a bluff-body using proper orthogonal decomposition, Combustion and Flame 159 (9) (2012) 2872–2882.
[107] W. D. York, D. W. Simons, Y. Fu, Operational flexibility of ge's f-class gas turbines with the dln2. 6+ combustion system, in: Turbo Expo: Power for Land, Sea, and Air, Vol. 51067, American Society of Mechanical Engineers, 2018, p. V04BT04A063.
[108] B. Kiel, K. Garwick, J. Gord, J. Miller, A. Lynch, R. Hill, S. Phillips, A detailed investigation of bluff body stabilized flames, in: 45th AIAA Aerospace Sciences Meeting and Exhibit, 2007, p. 168.
[109] S. M. Bush, E. J. Gutmark, Reacting and nonreacting flowfields of a v-gutter stabilized flame, AIAA Journal 45 (3) (2007) 662–672.
[110] B. Emerson, J. O'Connor, M. Juniper, T. Lieuwen, Density ratio effects on reacting bluff-body flow field characteristics, Journal of Fluid Mechanics 706 (2012) 219–250.
[111] B. L. Emerson, Dynamical characteristics of reacting bluff body wakes, Ph.D. thesis, Georgia Institute of Technology (2013).
[112] A. A. Chaparro, B. M. Cetegen, Blowoff characteristics of bluff-body stabilized conical premixed flames under upstream velocity modulation, Combustion and Flame 144 (1-2) (2006) 318–335.
[113] S. H. Hong, Towards predicting dynamics in turbulent premixed combustion using piv-plif measurements of flow-flame microstructure, Ph.D. thesis, Massachusetts Institute of Technology (2014).
[114] R. K. Cheng, et al., Low swirl combustion, The Gas Turbine Handbook (2006) 241–255.
[115] D. Kang, F. Culick, A. Ratner, Combustion dynamics of a low-swirl combustor, Combustion and Flame 151 (3) (2007) 412–425.
[116] M. Escudier, Vortex breakdown: observations and explanations, Progress in Aerospace Sciences 25 (2) (1988) 189–229.
[117] M. Hall, Vortex breakdown, Annual Review of Fluid Mechanics 4 (1) (1972) 195–218.
[118] T. Loiseleux, J. Chomaz, P. Huerre, The effect of swirl on jets and wakes: Linear instability of the rankine vortex with axial flow, Physics of Fluids 10 (5) (1998) 1120–1134.
[119] Z. Rusak, S. Wang, Review of theoretical approaches to the vortex breakdown phenomenon, in: Theroretical Fluid Mechanics Conference, 1996, p. 2126.
[120] M. Ruith, P. Chen, E. Meiburg, T. Maxworthy, Three-dimensional vortex breakdown in swirling jets and wakes: direct numerical simulation, Journal of Fluid Mechanics 486 (2003) 331–378.
[121] K. Manoharan, M. Frederick, S. Clees, J. O'Connor, S. Hemchandra, A weakly nonlinear analysis of the precessing vortex core oscillation in a variable swirl turbulent round jet, Journal of Fluid Mechanics 884 (2020).
[122] K. Oberleithner, C. O. Paschereit, R. Seele, I. Wygnanski, Formation of turbulent vortex breakdown: intermittency, criticality, and global instability, AIAA Journal 50 (7) (2012) 1437–1452.
[123] T. B. Benjamin, Theory of the vortex breakdown phenomenon, Journal of Fluid Mechanics 14 (4) (1962) 593–629.
[124] D. Darmofal, R. Khan, E. Greitzer, C. Tan, Vortex core behaviour in confined and unconfined geometries: a quasi-one-dimensional model, Journal of Fluid Mechanics 449 (2001) 61.
[125] Z. Rusak, Axisymmetric swirling flow around a vortex breakdown point, Journal of Fluid Mechanics 323 (1996) 79–105.
[126] Z. Rusak, C. Whiting, S. Wang, Axisymmetric breakdown of a q-vortex in a pipe, AIAA Journal 36 (10) (1998) 1848–1853.
[127] Z. Rusak, A. Kapila, J. J. Choi, Effect of combustion on near-critical swirling flow, Combustion The-

ory and Modelling 6 (4) (2002) 625–645.
[128] P. Moise, J. Mathew, Bubble and conical forms of vortex breakdown in swirling jets, Journal of Fluid Mechanics 873 (2019) 322–357.
[129] I. Chterev, C. Foley, D. Foti, S. Kostka, A. Caswell, N. Jiang, A. Lynch, D. Noble, S. Menon, J. Seitzman, et al., Flame and flow topologies in an annular swirling flow, Combustion Science and Technology 186 (8) (2014) 1041–1074.
[130] P. Huerre, P. A. Monkewitz, Local and global instabilities in spatially developing flows, Annual Review of Fluid Mechanics 22 (1) (1990) 473–537.
[131] C.-M. Ho, P. Huerre, Perturbed free shear layers, Annual Review of Fluid Mechanics 16 (1) (1984) 365–422.
[132] P. Huerre, P. A. Monkewitz, Absolute and convective instabilities in free shear layers, Journal of Fluid Mechanics 159 (1985) 151–168.
[133] B. Pier, P. Huerre, Nonlinear self-sustained structures and fronts in spatially developing wake flows, Journal of Fluid Mechanics 435 (2001) 145–174.
[134] P. A. Monkewitz, K. D. Sohn, Absolute instability in hot jets, AIAA Journal 26 (8) (1988) 911–916.
[135] L. K. Li, M. P. Juniper, Lock-in and quasiperiodicity in a forced hydrodynamically self-excited jet, Journal of Fluid Mechanics 726 (2013) 624–655.
[136] B. M. Cetegen, T. A. Ahmed, Experiments on the periodic instability of buoyant plumes and pool fires, Combustion and Flame 93 (1-2) (1993) 157–184.
[137] M.-H. Yu, P. A. Monkewitz, The effect of nonuniform density on the absolute instability of two-dimensional inertial jets and wakes, Physics of Fluids A: Fluid Dynamics 2 (7) (1990) 1175–1181.
[138] C. H. Williamson, Vortex dynamics in the cylinder wake, Annual Review of Fluid Mechanics 28 (1) (1996) 477–539.
[139] Y. Bury, T. Jardin, Transitions to chaos in the wake of an axisymmetric bluff body, Physics Letters A 376 (45) (2012) 3219–3222.
[140] P. Bohorquez, E. Sanmiguel-Rojas, A. Sevilla, J. Jiménez-González, C. Martínez-Bazán, Stability and dynamics of the laminar wake past a slender blunt-based axisymmetric body, Journal of Fluid Mechanics 676 (2011) 110–144.
[141] A. Prasad, C. H. Williamson, The instability of the shear layer separating from a bluff body, Journal of Fluid Mechanics 333 (1997) 375–402.
[142] D. Barkley, M. G. M. Gomes, R. D. Henderson, Three-dimensional instability in flow over a backward-facing step, Journal of Fluid Mechanics 473 (2002) 167–190.
[143] H. M. Blackburn, D. Barkley, S. J. Sherwin, Convective instability and transient growth in flow over a backward-facing step, Journal of Fluid Mechanics 603 (2008) 271–304.
[144] L. Kaiktsis, G. E. Karniadakis, S. A. Orszag, Unsteadiness and convective instabilities in two-dimensional flow over a backward-facing step, Journal of Fluid Mechanics 321 (1996) 157–187.
[145] H. M. Altay, R. L. Speth, D. E. Hudgins, A. F. Ghoniem, Flame–vortex interaction driven combustion dynamics in a backward-facing step combustor, Combustion and Flame 156 (5) (2009) 1111–1125.
[146] M. R. Gruber, J. M. Donbar, C. D. Carter, K.-Y. Hsu, Mixing and combustion studies using cavity-based flameholders in a supersonic flow, Journal of Propulsion and Power 20 (5) (2004) 769–778.
[147] K.-Y. Hsu, L. Goss, W. Roquemore, Characteristics of a trapped-vortex combustor, Journal of Propulsion and Power 14 (1) (1998) 57–65.
[148] S. Elder, Self-excited depth-mode resonance for a wall-mounted cavity in turbulent flow, The Journal of the Acoustical Society of America 64 (3) (1978) 877–890.
[149] F. Gallaire, J.-M. Chomaz, Instability mechanisms in swirling flows, Physics of Fluids 15 (9) (2003) 2622–2639.
[150] D. G. Lilley, Swirl flows in combustion: a review, AIAA Journal 15 (8) (1977) 1063–1078.
[151] H. Liang, T. Maxworthy, An experimental investigation of swirling jets, Journal of Fluid Mechanics 525 (2005) 115–159.
[152] N. Syred, A review of oscillation mechanisms and the role of the precessing vortex core (pvc) in swirl combustion systems, Progress in Energy and Combustion Science 32 (2) (2006) 93–161.
[153] P. Billant, J.-M. Chomaz, P. Huerre, Experimental study of vortex breakdown in swirling jets, Journal of Fluid Mechanics 376 (1998) 183–219.
[154] K. Oberleithner, C. O. Paschereit, I. Wygnanski, On the impact of swirl on the growth of coherent structures, Journal of Fluid Mechanics 741 (2014) 156–199.
[155] D. L. Kirkpatrick, Experimental investigation of the breakdown of a vortex in a tube, Aeronautical Research Council Current Papers (1965).
[156] S. Leibovich, K. Stewartson, A sufficient condition for the instability of columnar vortices, Journal of Fluid Mechanics 126 (1983) 335–356.
[157] J. Randall, S. Leibovich, The critical state: a trapped wave model of vortex breakdown, Journal of Fluid Mechanics 58 (3) (1973) 495–515.
[158] A. Albayrak, M. P. Juniper, W. Polifke, Propagation speed of inertial waves in cylindrical swirling flows, Journal of Fluid Mechanics 879 (2019) 85–120.
[159] J. S. Müller, F. Lückoff, T. L. Kaiser, C. O. Paschereit, K. Oberleithner, Modal decomposition and linear modeling of swirl fluctuations in the mixing section of a model combustor based on particle image velocimetry data, Journal of Engineering for Gas Turbines and Power 144 (1) (2022).
[160] C. Hirsch, D. Fanaca, P. Reddy, W. Polifke, T. Sattelmayer, Influence of the swirler design on the flame transfer function of premixed flames, in: Turbo Expo: Power for Land, Sea, and Air, Vol. 4725, 2005, pp. 151–160.
[161] C. Petz, H.-C. Hege, K. Oberleithner, M. Sieber, C. Nayeri, C. Paschereit, I. Wygnanski, B. Noack, Global modes in a swirling jet undergoing vortex breakdown, Physics of Fluids 23 (9) (2011) 091102.
[162] G. Berkooz, P. Holmes, J. L. Lumley, The proper orthogonal decomposition in the analysis of turbulent flows, Annual Review of Fluid Mechanics 25 (1) (1993) 539–575.
[163] J. Müller, F. Lückoff, P. Paredes, V. Theofilis, K. Oberleithner, Receptivity of the turbulent precessing vortex core: synchronization experiments and global adjoint linear stability analysis, Journal of Fluid Mechanics 888 (2020).
[164] S. Hemchandra, S. Shanbhogue, S. Hong, A. F. Ghoniem, Role of hydrodynamic shear layer stability in driving combustion instability in a premixed propane-air backward-facing step combustor, Physical Review Fluids 3 (6) (2018) 063201.

[165] S. R. Chakravarthy, O. J. Shreenivasan, B. Boehm, A. Dreizler, J. Janicka, Experimental characterization of onset of acoustic instability in a nonpremixed half-dump combustor, The Journal of the Acoustical Society of America 122 (1) (2007) 120–127.

[166] J.-M. Chomaz, Global instabilities in spatially developing flows: non-normality and nonlinearity, Annual Review of Fluid Mechanics 37 (2005) 357–392.

[167] F. Giannetti, P. Luchini, Structural sensitivity of the first instability of the cylinder wake, Journal of Fluid Mechanics 581 (2007) 167–197.

[168] M. P. Juniper, B. Pier, The structural sensitivity of open shear flows calculated with a local stability analysis, European Journal of Mechanics-B/Fluids 49 (2015) 426–437.

[169] K. Oberleithner, S. Schimek, C. O. Paschereit, Shear flow instabilities in swirl-stabilized combustors and their impact on the amplitude dependent flame response: A linear stability analysis, Combustion and Flame 162 (1) (2015) 86–99.

[170] S. Hong, R. L. Speth, S. J. Shanbhogue, A. F. Ghoniem, Examining flow-flame interaction and the characteristic stretch rate in vortex-driven combustion dynamics using piv and numerical simulation, Combustion and Flame 160 (8) (2013) 1381–1397.

[171] S. Hong, S. J. Shanbhogue, A. F. Ghoniem, Impact of fuel composition on the recirculation zone structure and its role in lean premixed flame anchoring, Proceedings of the Combustion Institute 35 (2) (2015) 1493–1500.

[172] J.-M. Chomaz, P. Huerre, L. G. Redekopp, A frequency selection criterion in spatially developing flows, Studies in Applied Mathematics 84 (2) (1991) 119–144.

[173] D. Crighton, M. Gaster, Stability of slowly diverging jet flow, Journal of Fluid Mechanics 77 (2) (1976) 397–413.

[174] P. A. Monkewitz, P. Huerre, J.-M. Chomaz, Global linear stability analysis of weakly non-parallel shear flows, Journal of Fluid Mechanics 251 (1993) 1–20.

[175] B. Mathews, S. Hansford, J. O'Connor, Impact of swirling flow structure on shear layer vorticity fluctuation mechanisms, in: Turbo Expo: Power for Land, Sea, and Air, Vol. 49750, American Society of Mechanical Engineers, 2016, p. V04AT04A026.

[176] F. Lückoff, T. L. Kaiser, C. O. Paschereit, K. Oberleithner, Mean field coupling mechanisms explaining the impact of the precessing vortex core on the flame transfer function, Combustion and Flame 223 (2021) 254–266.

[177] D. Mason, S. Clees, M. Frederick, J. O'Connor, The effects of exit boundary condition on precessing vortex core dynamics, in: Turbo Expo: Power for Land, Sea, and Air, Vol. 58622, American Society of Mechanical Engineers, 2019, p. V04BT04A009.

[178] J. O'Connor, T. Lieuwen, Further characterization of the disturbance field in a transversely excited swirl-stabilized flame, Journal of Engineering for Gas Turbines and Power 134 (1) (2012).

[179] J. O'Connor, T. Lieuwen, Influence of transverse acoustic modal structure on the forced response of a swirling nozzle flow, in: Turbo Expo: Power for Land, Sea, and Air, Vol. 44687, American Society of Mechanical Engineers, 2012, pp. 1491–1503.

[180] M. Hauser, M. Lorenz, T. Sattelmayer, Influence of transversal acoustic excitation of the burner approach flow on the flame structure, Journal of Engineering for Gas Turbines and Power 133 (4) (2011) 041501.

[181] J. R. Dawson, N. A. Worth, Flame dynamics and unsteady heat release rate of self-excited azimuthal modes in an annular combustor, Combustion and Flame 161 (10) (2014) 2565–2578.

[182] A. Saurabh, C. O. Paschereit, Dynamics of premixed swirl flames under the influence of transverse acoustic fluctuations, Combustion and Flame 182 (2017) 298–312.

[183] A. Saurabh, J. P. Moeck, C. O. Paschereit, Swirl flame response to simultaneous axial and transverse velocity fluctuations, Journal of Engineering for Gas Turbines and Power 139 (6) (2017) 061502.

[184] J. O'Connor, Response of a swirl-stabilized flame to transverse acoustic excitation, Ph.D. thesis, Georgia Institute of Technology (2011).

[185] J. O'Connor, T. Lieuwen, Recirculation zone dynamics of a transversely excited swirl flow and flame, Physics of Fluids 24 (7) (2012) 2893–2900.

[186] F. Gallaire, J.-M. Chomaz, Mode selection in swirling jet experiments: a linear stability analysis, Journal of Fluid Mechanics 494 (2003) 223–253.

[187] A. Karmarkar, A. Tyagi, S. Hemchandra, J. O'Connor, Impact of turbulence on the coherent flame dynamics in a bluff-body stabilized flame, Proceedings of the Combustion Institute 38 (2) (2021) 3067–3075.

[188] B. F. Farrell, P. J. Ioannou, Stochastic forcing of the linearized navier–stokes equations, Physics of Fluids A: Fluid Dynamics 5 (11) (1993) 2600–2609.

[189] S. J. Shanbhogue, M. Seelhorst, T. Lieuwen, Vortex phase-jitter in acoustically excited bluff body flames, International Journal of Spray and Combustion Dynamics 1 (3) (2009) 365–387.

[190] N. Cumpsty, F. Marble, The interaction of entropy fluctuations with turbine blade rows; a mechanism of turbojet engine noise, Proceedings of the Royal Society of London. A. Mathematical and Physical Sciences 357 (1690) (1977) 323–344.

[191] N. Bunce, Flame transfer function measurements and mechanisms in a single-nozzle combustor, Ph.D. thesis, Pennsylvania State University (2013).

[192] R. Erickson, M. Soteriou, The influence of reactant temperature on the dynamics of bluff body stabilized premixed flames, Combustion and Flame 158 (12) (2011) 2441–2457.

[193] S. Rees, M. Juniper, The effect of confinement on the stability of viscous planar jets and wakes, Journal of Fluid Mechanics 656 (2010) 309–336.

[194] B. L. Emerson, D. R. Noble, T. C. Lieuwen, Stability analysis of reacting wakes: The physical role of flame-shear layer offset, in: 52nd Aerospace Sciences Meeting, 2014, p. 0659.

[195] K. Oberleithner, S. Terhaar, L. Rukes, C. Oliver Paschereit, Why nonuniform density suppresses the precessing vortex core, Journal of Engineering for Gas Turbines and Power 135 (12) (2013).

[196] K. Oberleithner, M. Stöhr, S. H. Im, C. M. Arndt, A. M. Steinberg, Formation and flame-induced suppression of the precessing vortex core in a swirl combustor: experiments and linear stability analysis, Combustion and Flame 162 (8) (2015) 3100–3114.

[197] S. Terhaar, K. Oberleithner, C. O. Paschereit, Key parameters governing the precessing vortex core in reacting flows: An experimental and analytical study, Proceedings of the Combustion Institute 35 (3)

(2015) 3347–3354.
[198] M. Stöhr, K. Oberleithner, M. Sieber, Z. Yin, W. Meier, Experimental study of transient mechanisms of bistable flame shape transitions in a swirl combustor, Journal of Engineering for Gas Turbines and Power 140 (1) (2018).
[199] J. P. Moeck, J.-F. Bourgouin, D. Durox, T. Schuller, S. Candel, Nonlinear interaction between a precessing vortex core and acoustic oscillations in a turbulent swirling flame, Combustion and Flame 159 (8) (2012) 2650–2668.
[200] L. Crocco, Research on combustion instability in liquid propellant rockets, Symposium (International) on Combustion 12 (1) (1969) 85–99.
[201] K. T. Kim, S. Hochgreb, Measurements of triggering and transient growth in a model lean-premixed gas turbine combustor, Combustion and Flame 159 (3) (2012) 1215–1227.
[202] A. Urbano, L. Selle, G. Staffelbach, B. Cuenot, T. Schmitt, S. Ducruix, S. Candel, Exploration of combustion instability triggering using large eddy simulation of a multiple injector liquid rocket engine, Combustion and Flame 169 (2016) 129–140.
[203] M. Bauerheim, F. Nicoud, T. Poinsot, Progress in analytical methods to predict and control azimuthal combustion instability modes in annular chambers, Physics of Fluids 28 (2) (2016) 021303.
[204] V. S. Acharya, M. R. Bothien, T. C. Lieuwen, Nonlinear dynamics of thermoacoustic eigen-mode interactions, Combustion and Flame 194 (2018) 309–321.
[205] N. Purwar, M. Haeringer, B. Schuermans, W. Polifke, Flame response to transverse velocity excitation leading to frequency doubling and modal coupling, Combustion and Flame 230 (2021) 111412.
[206] B. Emerson, T. Lieuwen, Dynamics of harmonically excited, reacting bluff body wakes near the global hydrodynamic stability boundary, Journal of Fluid Mechanics 779 (2015) 716–750.
[207] S. A. Pawar, R. I. Sujith, B. Emerson, T. Lieuwen, Characterization of forced response of density stratified reacting wake, Chaos: An Interdisciplinary Journal of Nonlinear Science 28 (2) (2018) 023108.
[208] C. O. Paschereit, E. Gutmark, W. Weisenstein, Excitation of thermoacoustic instabilities by interaction of acoustics and unstable swirling flow, AIAA Journal 38 (6) (2000) 1025–1034.
[209] A. Lacarelle, T. Faustmann, D. Greenblatt, C. Paschereit, O. Lehmann, D. Luchtenburg, B. Noack, Spatiotemporal characterization of a conical swirler flow field under strong forcing, Journal of Engineering for Gas Turbines and Power 131 (3) (2009).
[210] P. Iudiciani, C. Duwig, Large eddy simulation of the sensitivity of vortex breakdown and flame stabilisation to axial forcing, Flow, Turbulence and Combustion 86 (3) (2011) 639–666.
[211] A. M. Steinberg, I. Boxx, M. Stöhr, C. D. Carter, W. Meier, Flow–flame interactions causing acoustically coupled heat release fluctuations in a thermoacoustically unstable gas turbine model combustor, Combustion and Flame 157 (12) (2010) 2250–2266.
[212] R. Zhang, I. Boxx, W. Meier, C. D. Slabaugh, Coupled interactions of a helical precessing vortex core and the central recirculation bubble in a swirl flame at elevated power density, Combustion and Flame 202 (2019) 119–131.
[213] A. Karmarkar, S. Gupta, I. Boxx, S. Hemchandra, J. O'Connor, Impact of precessing vortex core dynamics on the thermoacoustic instabilities in a swirl stabilized combustor, arXiv preprint arXiv:2011.14662 (2020).
[214] A. Towne, O. T. Schmidt, T. Colonius, Spectral proper orthogonal decomposition and its relationship to dynamic mode decomposition and resolvent analysis, Journal of Fluid Mechanics 847 (2018) 821–867.
[215] M. P. Juniper, Absolute and convective instability in gas turbine fuel injectors, in: Turbo Expo: Power for Land, Sea, and Air, Vol. 44687, American Society of Mechanical Engineers, 2012, pp. 189–198.
[216] K. Oberleithner, M. Sieber, C. N. Nayeri, C. O. Paschereit, C. Petz, H.-C. Hege, B. R. Noack, I. Wygnanski, Three-dimensional coherent structures in a swirling jet undergoing vortex breakdown: stability analysis and empirical mode construction, Journal of Fluid Mechanics 679 (2011) 383–414.
[217] O. Tammisola, M. P. Juniper, Adjoint sensitivity analysis of hydrodynamic stability in a gas turbine fuel injector, in: Turbo Expo: Power for Land, Sea, and Air, Vol. 56680, American Society of Mechanical Engineers, 2015, p. V04AT04A057.
[218] K. Zaman, J. Bridges, D. Huff, Evolution from 'tabs' to 'chevron technology'-a review, International Journal of Aeroacoustics 10 (5-6) (2011) 685–709.
[219] L. Kaiktsis, P. A. Monkewitz, Global destabilization of flow over a backward-facing step, Physics of Fluids 15 (12) (2003) 3647–3658.
[220] C. O. Paschereit, E. J. Gutmark, Control of high-frequency thermoacoustic pulsations by distributed vortex generators, AIAA Journal 44 (3) (2006) 550–557.
[221] H. M. Altay, D. E. Hudgins, R. L. Speth, A. M. Annaswamy, A. F. Ghoniem, Mitigation of thermoacoustic instability utilizing steady air injection near the flame anchoring zone, Combustion and Flame 157 (4) (2010) 686–700.
[222] I. Boxx, C. M. Arndt, C. D. Carter, W. Meier, High-speed laser diagnostics for the study of flame dynamics in a lean premixed gas turbine model combustor, Experiments in Fluids 52 (3) (2012) 555–567.
[223] H. Mongia, T. Held, G. Hsiao, R. Pandalai, Incorporation of combustion instability issues into design process: Ge aeroderivative and aero engines experience, Progress in Astronautics and Aeronautics 210 (2005) 43.
[224] T. Poinsot, Prediction and control of combustion instabilities in real engines, Proceedings of the Combustion Institute 36 (1) (2017) 1–28.